Asynchronous sampled-data String Stability for a platoon of heterogeneous vehicles via a mesoscopic approach

Mattia Mattioni, Alessio Iovine

Asynchronous sampled-data String Stability for a platoon of heterogeneous vehicles via a mesoscopic approach

Mattia Mattioni, *Member, IEEE*, Alessio Iovine, *Member, IEEE*

***Abstract*—This paper proposes a new mesoscopic approach for controlling a platoon of vehicles under asynchronous sampled-data measurements and bounded disturbances. The proposed control law yields disturbance string stability independently of the effect of sampling. The design is constructive and yields simple-to-check conditions to enforce good performance and safety. Simulations illustrate the theoretical results.**

***Index Terms*—Traffic control, Sampled data control, String stability, Agents and autonomous systems.**

I. Introduction

SOPHISTICATED control techniques for Intelligent Transportation Systems (ITS) are fundamental to meet the rising need for enhanced transportation efficiency and improved safety [1]–[5]. These methods are required to handle the intricate and dynamic nature of ITS, where various agents interact with each other and the environment. The potential utilization of Connected Autonomous Vehicles (CAV) implementing Cooperative Adaptive Cruise Controllers (CACC) adds another dimension of complexity to achieving these objectives. In this framework, current research literature is focusing on enforcing a fundamental property for developing efficient and safe CACC, that is String Stability (SS, [2], [3], [6], [7]). Roughly speaking, the latter concept refers to the ability of a series of vehicles in a platoon, or *string*, to maintain a target distance between each other while moving along a roadway and not amplifying the effect of disturbances over the states.

As one might expect, the kind of information that is exchanged over the platoon is of paramount importance to enforce SS. Historically, various instances of such information exchange have been investigated under the standard leader-follower interaction; namely, each vehicle $i \in \mathbb{N}$ of the platoon is considered a follower with respect to the vehicle ahead (or predecessor, say $i-1$). In this context, each follower vehicle is supposed to measure or receive the so-called microscopic information on the corresponding predecessor and of the leader of the whole platoon (that is the primer vehicle). In particular, each vehicle must receive full measures on the preceding vehicle (i.e., the speed, the relative position and, possibly, the acceleration) whereas only partial information is required from the platoon leader (e.g., its acceleration [6] or desired speed profile [8]). The communication of the leader's information across the entire platoon represents a demanding shared trait to put into practice [9]. In contrast to conventional leader-follower scenarios, even more demanding platooning configurations in terms of information exchange are termed Multiple-Predecessor Following (MPF, [10], [11]). Indeed, these configurations involve exchanging information with a group of ahead vehicles, thus resulting in an increased amount of communication for performance purposes. However, this setup does not resolve the challenge of identifying a distinct leader and sharing its information with the whole platoon (e.g., speed profile in [11]). It makes the information exchange process more involved as it demands for sharing of several quantities (e.g., acceleration, speed and relative position) over the whole group of vehicles, usually via Vehicle-to-Vehicle (V2V) communications.

Recently, further investigations have been devoted to exploring the possibility of ensuring desired properties, such as SS, making use of macroscopic information. This is realized by considering, for instance, Vehicle-to-Infrastructure (V2I) communications. In this setting, the goal is to minimize the exchange of information over the platoon by avoiding sharing microscopic details of the primer vehicle while reducing the dimension and complexity of the dynamical models to consider. This is achieved by relying on suitable aggregate information, which can be shared through either V2I (that is commonly preferred) or V2V communication [12]–[14]. More in detail, it was proved in [12] that SS can be enforced over a platoon via the use of local microscopic measures (i.e., on the vehicle ahead) and aggregate (macroscopic) information on the platoon solely. The corresponding control law is thus mesoscopic. In particular, the microscopic information available to each vehicle consists of the state of its predecessor only, while the macroscopic information is granted via V2V communications. In [13], those results were extended to the case in which disturbances affect both the vehicles and the information that is shared along the platoon. This results in the possibility of considering averaged macroscopic information, instead of tailored one as in [12], that is obtained by a smart traffic infrastructure and

Mattia Mattioni is with Dipartimento di Ingegneria Informatica, Automatica e Gestionale *A. Ruberti* (Università degli Studi di Roma *La Sapienza*); Via Ariosto 25, 00185 Rome, Italy. `mattioni@diag.uniroma1.it`

Alessio Iovine is with the Laboratory of Signal and Systems (L2S), Centre National de la Recherche Scientifique (CNRS), CentraleSupélec, Paris-Saclay University, 3, rue Joliot-Curie, 91192 Gif-sur-Yvette, France. E-mail: `alessio.iovine@centralesupelec.fr`

shared via V2I communication. In [14], a link between the possibility of ensuring SS and the way the traffic Fundamental Diagram is impacted was proposed. Other works focus on mesoscopic modeling for traffic control purposes, e.g., [15]–[20]. However, no formal SS analysis is usually performed (see [17], [19], [20]); if any, such analysis is based on the linear tangent model only (see [15], [16]).

The theoretical results in [12]–[14], as well as most of the available literature on mesoscopic or multi-scale traffic models [21]–[23], concern continuous-time systems only; i.e., when measurements and the information on the traffic flow are available continuously in time and the control input arbitrarily varies at all times. This framework is far from being realistic as it does not take into account the discrete-time influence of digital devices, which are unavoidable for control implementation and in the way the information exchange is realized within the platoon. This limitation highlights the necessity for sampled-data approaches in CACC; namely, when measures are sampled and available only at sporadic time instants (the so-called sampling instants) and the control inputs are piecewise constant over the sampling period [24]–[27].

In this scenario, only few results are available and, however, usually refer to the so-called *emulation-based control*; namely, the controller is designed by completely neglecting the effect of sampling and then implemented in practice via sample-and-hold devices (see, among many, [28], [29] for a general overview, and [30], [31] for applications to a similar context). As the intuition might suggest, those kinds of control laws preserve the same performances enforced by the continuous-time (nominal) design only when the involved sampling periods are very small. Contrarily to the aforementioned approaches, referring to a discrete-time problem formulation, a new simple controller has been proposed in [32] to enforce string stability across the platoon despite the effect of sampling, i.e., independently on the length of the involved sampling periods. This is done when assuming that all vehicles receive both micro and macro measurements synchronously in time. In addition, no disturbance has been considered in the design.

This paper aims to make further steps toward this direction by considering a heterogeneous platoon of vehicles, thus allowing measures to be asynchronous for each vehicle and bounded disturbances affect the whole platoon. More in detail, each vehicle receives both the microscopic and macroscopic information at intermittent time instants, which may not be uniformly synchronized across the entire platoon. Moreover, the macroscopic information is received less frequently than the microscopic one; the time instances at which the former is available constitute a subset of the sampling moments for micro-information measures. This scenario is grounded in reality, accounting for a diverse array of vehicles engaging with both one another and the smart traffic infrastructure capturing and sharing the macroscopic information through V2I communications at varying sampling intervals.

With this in mind, the local control we propose for each vehicle enforces Disturbance String Stability (DSS) over the platoon [8], despite the effect of sampling and holding devices. The design is constructive and we provide simple conditions allowing to define, independently on the length of the involved sampling periods, the stabilizing controller. Such conditions allow guaranteeing good performances in terms of tracking the desired intervehicular distance and speed profiles while ensuring safety and avoiding disturbance propagation along the platoon. More in detail, under mild assumptions on the macroscopic functions that can be considered, we provide a general dynamic mesoscopic control law capable of enforcing DSS across the platoon. The proposed control law is generated by a discrete-time system, one per vehicle, working at the corresponding sampling instants. The dimension and structure of each controller are left free as they account for the particular mesoscopic spacing policies at hand and the way the macro-information is measured by each vehicle. The design is then specified to two distinct classes of spacing policies: the constant one, which is classically adopted, with a controller considering macroscopic information; and a mesoscopic one, which embeds the constant spacing policy with macroscopic conditions. To the best of the Authors' knowledge, no results are available for solving the problem in this scenario, despite its significance in applications.

The rest of the paper is organized as follows. Section II provides the considered models and hypothesis, as well as the problem statement. Section III introduces the main result with respect to different spacing policies. Section IV shows the effectiveness of the proposed sampled-data solution in simulations, while Section V outlines concluding remarks. We underline that the proof of the main result and the required instrumental tools are reported in Appendix for the sake of reading.

Notations

$\mathbb{C}$, $\mathbb{R}$ and $\mathbb{N}$ denote the set of complex, real and natural numbers including 0 respectively. $\mathbb{R}^+$ denotes the set of positive real numbers. I and 0 denote respectively the identity and zero matrices of suitable dimensions. Given a matrix $A \in \mathbb{R}^{n\times n}$, $\sigma\{A\} \subset \mathbb{C}$ is its spectrum. For a complex number $\lambda \in \mathbb{C}$, $\mathrm{Re}\{\lambda\}$ denotes its real part. A is said to be Schur if its spectrum is included in the open unit circle of the complex plane (i.e., all its eigenvalues are with norm strictly less than 1 and none is at the origin). $|\cdot| \in \mathbb{R}$ denotes, depending on the argument, either the cardinality of a set $\mathcal{S}$, the absolute value of a complex number $\lambda \in \mathbb{C}$ or the norm of a matrix. Given a continuous-time signal $w : \mathbb{R}_{\geq 0} \to \mathbb{R}$ we define $\|w\|^{[0,\bar{t})} := \sup_{t\in[0,\bar{t})} |w(t)|$. Similarly, for a discrete-time signal $w_d : \mathbb{N} \to \mathbb{R}$ we define $\|w_d\|^{\{0,\dots,\bar{k}\}} := \sup_{k\in[0,\bar{k})} |w_d(k)|$; when the discrete signal is deduced by sampling a continuous-time signal $w(t)$ (i.e., $w_d(k) = w(t_k)$ for $t_k \in \mathbb{R}$ and $k \in \mathbb{N}$) we denote $\|w_d\|^{\{0,\dots,\bar{k}\}} = \|w(t_k)\|^{\{0,\dots,\bar{k}\}}$. Given N matrices $B_i \in \mathbb{R}^{n_i\times m}$ of suitable dimensions, we denote

$$\mathrm{col}\{B_1,\dots,B_N\} = \begin{bmatrix} B_1^\top & \dots & B_n^\top \end{bmatrix}^\top \in \mathbb{R}^{(n_1+\dots+n_N)\times m}.$$

$1_N = \mathrm{col}\{1,\dots,1\} \in \mathbb{R}^N$ is the vector with all entries being one. "$\otimes$" denotes the Kronecker product.

II. Modeling and Problem formulation

A. Microscopic modeling

Let $\mathcal{I}_0^N$ be the set of N vehicles composing a platoon. Each vehicle is described by its longitudinal position, $p_i \in \mathbb{R}^+$, and its longitudinal speed, $0 \leq v_i \leq v_{\max}$, $v_{\max} \in \mathbb{R}^+$, $\forall\, i \in \mathcal{I}_0^N$. Then, we define the state of the $i-$th vehicle as $x_i = \text{col}\{p_i,\ v_i\}$. Without loss of generality, the low-level dynamics describing the power-train can be considered to have been feedback linearised (see [6], [8], [33]), thus allowing for a simplification in considering only the longitudinal dynamics for describing heterogeneous platoons [34], i.e., platoons composed by non identical vehicles. The corresponding dynamical system is obtained [6], [33], [35], [36]:

$$\dot{x}_i = \text{col}\{\dot{p}_i,\ \dot{v}_i\} = \text{col}\{v_i, u_i + \tilde{d}_i\}, \qquad i \in \mathcal{I}_0^N, \tag{1}$$

where: $|u_i| \leq u_{\max}$, $u_{\max} \in \mathbb{R}^+$, is the control input of the $i-$th vehicle, corresponding to the acceleration; $\tilde{d}_i \in \mathbb{R}$ is a disturbance. To describe inter-vehicular interactions, we adopt the leader-follower model (see [37]) to derive a global description of the platoon. For the derived model to include vehicle $i = 0$, we consider the presence of a virtual leader, $i = -1$, that precedes the entire platoon, with dynamical model

$$\dot{x}_{-1} = \text{col}\{\dot{p}_{-1},\ \dot{v}_{-1}\} = \text{col}\{v_{-1},\ u_{-1} + \tilde{d}_{-1}\} \tag{2}$$

where $u_{-1} = \tilde{d}_{-1} \equiv 0$. Then, the state of each car-following situation between vehicles $i-1$ and i is

$$\chi_i = x_i - x_{i-1} = \text{col}\{\Delta p_i,\ \Delta v_i\} = \text{col}\{p_i - p_{i-1},\ v_i - v_{i-1}\} \tag{3}$$

for $i \in \mathcal{I}_0^N$. The resulting microscopic dynamical model of the $i-$th car-following pair is

$$\dot{\chi}_i = A\chi_i + B\left(u_i - u_{i-1} + d_i\right),\ \ i \in \mathcal{I}_0^N \tag{4}$$

with $d_i := \tilde{d}_i - \tilde{d}_{i-1}$ and

$$A = \begin{bmatrix} 0 & 1 \\ 0 & 0 \end{bmatrix}, \quad B = \begin{bmatrix} 0 \\ 1 \end{bmatrix}. \tag{5}$$

Remark 1: The approach we propose can be applied to third-order models embedding further components describing, for instance, jerk or torque dynamics as in [37], [38]. Without loss of generality, the second-order model at hand is sufficiently realistic as recognized in several seminal works as [8], [36], [39].

To each vehicle $i \in \mathcal{I}_0^N$ we associate the sampling sequence $\Delta_i := \{t_{0_i}, t_{1_i}, \dots, t_{k_i}, \dots\}$ with $t_{k_i+1} - t_{k_i} := T_i$ $T_i > 0$. In the following, we denote maximum sampling period as $T_{\max} = \max_{i \in \mathcal{I}_0^N}\{T_i\}$. At this point, the following assumption is set.

Assumption 1 (Microscopic sampling): The input u_i of each vehicle $i \in \mathcal{I}_0^N$ is a piecewise constant signal over the sampling period of length $T_i \geq 0$, that is

$$u_i(t) = u_i(t_{k_i}), \quad t \in [t_{k_i}, t_{k_i+1}) \text{ and } t_{k_i}, t_{k_i+1} \in \Delta_i. \tag{6}$$

In addition, each vehicle $i \in \mathcal{I}_0^N$ measures its corresponding microscopic quantities x_i, x_{i-1}, u_{i-1} at all $t_{k_i} \in \Delta_i$.

Remark 2: The assumption above requires that each vehicle can estimate the control acceleration of its predecessor. This scenario is not far from reality due to the on-board sensors modern vehicles implementing CACC are prototyped with, e.g., LiDAR. In addition, further uncertainties in the measurements of $u_{i-1}(t_{k_i})$ can be included in the disturbance term d_i by expressing u_{i-1} as the sum of a known component $\tilde{u}_{i-1}$ and a bounded disturbance $\hat{d}_i$, i.e., $u_{i-1} = \tilde{u}_{i-1} + \hat{d}_{i-1}$. Then, we can define the disturbance d_i as the sum of the uncertainties associated with both the disturbance and the microscopic control input: $d_i = \tilde{d}_i - \tilde{d}_{i-1} - \hat{d}_{i-1}$.

Under Assumption 1, the dynamics of each vehicle (4) at all sampling instants $t_{k_i} \in \Delta_i$ is described by the corresponding sampled-data equivalent model. For deducing it, we first note that, with no loss of generality, one can rewrite the sampling period of each vehicle $i \in \mathcal{I}_0^N$ in terms of the one of its predecessor setting

$$T_i = \mu_i T_{i-1} + \sigma_i, \quad \mu_i \in \mathbb{N}, \quad \sigma_i \in [0, T_{i-1}). \tag{7}$$

At this point, defining the sequence

$$\begin{aligned} \Delta_{k_i}^{i-1} :=& \{t_{k_i}^0, \dots, t_{k_i}^{\mu_i - 1}\} := [t_{k_i}, t_{k_i+1}) \cap \Delta_{i-1} \\ =& \{t_{k_{i-1}} \in \Delta_{i-1} \text{ s.t. } t_{k_{i-1}} \in [t_{k_i}, t_{k_i+1})\} \end{aligned} \tag{8}$$

the sampled-data equivalent model associated to each (4) [40] is given by

$$\chi_i(t_{k_i+1}) = A_i\chi_i(t_{k_i}) + B_i\big(u_i(t_{k_i}) - u_{i-1}(t_{k_i})\big) + f_i(t_{k_i}) \tag{9}$$

with setting $u_{i-1}(t_{k_i}^{-1}) := u_{i-1}(t_{k_i})$

$$A_i = e^{AT_i} = \begin{bmatrix} 1 & T_i \\ 0 & 1 \end{bmatrix},\ B_i = \int_0^{T_i} e^{A\ell}\mathrm{d}\ell B = \begin{bmatrix} \frac{T_i^2}{2} \\ T_i \end{bmatrix} \tag{10a}$$

$$\begin{aligned} f_i(t_{k_i}) = &\int_0^{T_i} e^{As} B d_i(t_{k_i+1} - s)\mathrm{d}s \\ &+ \sum_{r=0}^{\mu_i} D_i^r\big(u_{i-1}(t_{k_i}^{r-1}) - u_{i-1}(t_{k_i})\big) \end{aligned} \tag{10b}$$

$$D_i^r = \begin{cases} \int_{t_{k_i}}^{t_{k_i}^0} e^{A(t_{k_i+1} - \ell)}\mathrm{d}\ell B & r = 0 \\ e^{A(t_{k_i+1} - t_k^r)} B_{i-1} & r \in \{1, \dots, \mu_i - 1\} \\ \int_{t_{k_i}^{\mu_i - 1}}^{t_{k_i+1}} e^{A(t_{k_i+1} - \ell)}\mathrm{d}\ell B, & r = \mu_i. \end{cases} \tag{10c}$$

In the following, we will refer to (9) as the microscopic sampled-data equivalent model of (4).

Remark 3: The sequence (8) collects the time instants over the sampling interval $[t_{k_i}, t_{k_i+1})$ associated to vehicle i in which its predecessor updates the corresponding u_{i-1}.

Remark 4: The sampled-data model (9) is deduced by integrating each vehicle (4) over the corresponding sampling period $[t_{k_i}, t_{k_{i+1}})$. Thus, one can rewrite

$$\begin{aligned} &\sum_{r=0}^{\mu_i} D_i^r\big(u_{i-1}(t_{k_i}^{r-1}) - u_{i-1}(t_{k_i})\big) \\ &\qquad = \int_{t_{k_i}}^{t_{k_i+1}} e^{A(t_{k_i+1} - s)} B\big(u_{i-1}(t_{k_i}) - u_{i-1}(s)\big)\mathrm{d}s \end{aligned}$$

by partitioning

$$[t_{k_i}, t_{k_{i+1}}) = [t_{k_i}, t^0_{k_i}) \cup \Big(\cup_{r=1}^{\mu_i - 1} [t^{r-1}_{k_i}, t^r_{k_i}) \Big) \cup [t^{\mu-1}_{k_i}, t_{k_i+1}).$$

Thus, the effect of the asynchronism among two successive vehicles is modeled as a further disturbance affecting the state evolution. It is clear that when $T_i = T_{i-1}$ (i.e., $\Delta_i \equiv \Delta_{i-1}$) then $\mu_i = 1$, $\sigma_i = 0$, $D^r_i = B_i = B_{i-1}$, $u_{i-1}(t_{k_i}) = u_{i-1}(t_{k_{i-1}})$ and all such perturbing terms vanish.

Remark 5: For the sake of simplicity and without loss of generality, the control input $u_{i-1}(t_{k_i})$ is supposed to be measured at the same sampling instant as $u_i(t_{k_i})$ by the follower vehicle. Potential discrepancies compared to the scenario involving $u_{i-1}(t_{k_{i-1}})$ can be accounted for by incorporating the deviation from the nominal case into the disturbance term $f_i(t_{k_i})$.

Recalling that $u_{-1} = \tilde{d}_{-1} \equiv 0$, speed of the virtual leader (2) defines the reference speed for $i = 0$ [8], [12], [13]. Letting $\Delta\bar{p} > 0$ be the desired inter-vehicular distance at steady-state and setting

$$\Delta p_0(t_{k_0}) = -\Delta\bar{p} \quad \forall\, t_{k_0} \in \Delta_0, \tag{11}$$

then the equilibrium point for the $i-$th system of dynamics (4) corresponds to the case where all the vehicles are at the same distance with the same speed, i.e.,

$$\chi_{e,i} = \bar{\chi} := \text{col}\{-\Delta\bar{p},\ 0\},\ \forall\, i \in \mathcal{I}^N_0. \tag{12}$$

Since the state vector (3) is defined with respect to the follower vehicle, then the distance Δp_i and the relative speed Δv_i have opposite signs. For this reason, the equilibrium distance in (12) is $-\Delta\bar{p} < 0$. From the platoon point of view, we define the lumped state and the lumped equilibrium respectively as $\chi = \text{col}\{\chi_0,\ \dots,\ \chi_N\}$, $\chi_e = 1_N \otimes \bar{\chi}$.

B. Macroscopic modeling

In general, each vehicle $i \in \mathcal{I}^N_0$ receives a measure synthesizing the information on the platoon including all preceding vehicles $j \in \{0, 1, \dots, i-1\}$. More in detail, for all $i \in \mathcal{I}^N_0$, such an information is endowed within the so-called *macroscopic* function

$$\psi_{i-1}(\chi_0, \dots, \chi_{i-1}) : \mathbb{R}^2 \times \cdots \times \mathbb{R}^2 \to \mathbb{R}^2 \tag{13}$$

with, for $i = 0$, $\psi_{-1} = 0$, verifying for all $i \in \mathcal{I}^N_0$

$$|\psi_{i-1}(\chi_0, \dots, \chi_{i-1})| \leq \kappa \sum_{j=0}^{i-1} |\chi_j - \chi_{e,j}| \tag{14}$$

for some positive constant $\kappa \in \mathbb{R}$ and $\psi_{i-1}(\chi_{e,1}, \dots, \chi_{e,i-1}) = 0$ only. The purpose of the function ψ_{i-1} is to furnish the i-th vehicle with aggregate macroscopic information about the platoon system. These functions portray the state of the leading vehicles, signifying the presence of either a transient or a steady-state phase. As a result, equilibrium in the leading vehicles corresponds to a situation without oscillations. Compared to MPF approaches, this one does not encompass the entire set of leader-follower scenarios, providing a complexity reduction in the considered interconnection framework without compromising the available information level.

In the following, we let this quantity be spread over the network only at sporadic and intermittent time instants that are not the same as the ones of the microscopic measures (Assumption 1). To this end, we denote by $\Delta^M_i = \{t_{0^M_i}, t_{1^M_i}, \dots, t_{k^M_i}, \dots\} \subseteq \Delta_i$ the macroscopic sampling sequence with $t_{k^M_i+1} - t_{k^M_i} = mT_i$ for $m \in \mathbb{N}\backslash\{0\}$.

Assumption 2 (Macroscopic sampling): Each vehicle $i \in \mathcal{I}^N_0$ measures the macroscopic information function (13) at all $t \in t_{k^M_i} \in \Delta^M_i$ with corresponding sampling period $T^M_i := mT_i = t_{k^M_i+1} - t_{k^M_i}$ for some $m \in \mathbb{N}\backslash\{0\}$.

In the following, for all $i \in \mathcal{I}^N_0$, we shall refer to $t_{k_i} \in \Delta_i$ and $t_{k^M_i} \in \Delta_i$ as the microscopic and macroscopic sampling instants respectively. Similarly, T_i and T^M_i are called microscopic and macroscopic sampling periods. Thus, each vehicle defines a sampled-data asynchronous dynamics with the macroscopic and microscopic information available, in general, at different sampling instants. Finally, for the sake of compactness, we write

$$\psi_{i-1}(t^M_{k_i}) = \psi_{i-1}(\chi_0(t^M_{k_i}), \dots, \chi_{i-1}(t^M_{k_i})).$$

Remark 6: Our results cover $T^M_i = mT_i + \sigma^M_i$ with $m \in \mathbb{N}$ and $\sigma^M_i \in [0, T_i)$. This endows a traffic manager, (see [41]) that either shares a tailored macroscopic function, updated specifically at each $t^M_{k_i} \in \Delta^M_i$, or a common macroscopic function for the entire set of vehicles, updated with a constant rate but read by each vehicle at its macroscopic sampling instant.

C. Problem statement

We define the following *spacing policy*

$$\Delta p^r_i(t_{k_i}) = -\Delta\bar{p} - \rho_{\mathtt{m},i}(t_{k_i}),\ t_{k_i} \in \Delta_i \tag{15}$$

where $\Delta\bar{p}$ is the target constant inter-vehicular distance in (11), and $\rho_{\mathtt{m},i} \in \mathbb{R}$ is a function that is related to the macroscopic information received by each vehicle. In (15), the macroscopic contribution plays the role of adapting the spacing policy to current traffic conditions, similarly to other spacing policies that depend on vehicles' speed or desired time headway.

Under Assumptions 1 and 2, the objective of the paper is to deduce a piecewise constant dynamic controller asymptotically tracking the desired distance (11) based on asynchronous micro and macroscopic information.

More in detail, for all $t_{k_i} \in \Delta_i$ and $t_{k^M_i} \in \Delta^M_i$, we propose a dynamic sampled-data controller of the form

$$\begin{aligned} \rho_i(t_{k_i+1}) =& F_{\rho_i}\rho_i(t_{k_i}) + G_{e_i}e_i(t_{k_i}) + P_i\psi_{i-1}(t_{k^M_i}) \\ u_i(t_{k_i}) =& u_{i-1}(t_{k_i}) + H_{\rho_i}\rho_i(t_{k_i}) + H_{e_i}e_i(t_{k_i}) \\ &+ R_i\psi_{i-1}(t_{k^M_i}) \end{aligned} \tag{16}$$

where: $\rho_i \in \mathbb{R}^{n_\rho}$ is of suitable dimension $n_\rho \in \mathbb{N}$ and such that $\rho_i(0) = 0$; $e_i = \chi_i - \chi_{e,i} + Q_i\rho_i$ with $Q_i \in \mathbb{R}^{2\times n_\rho}$ such that $Q_i\rho_i = \text{col}\{\rho_{\mathtt{m},i}, 0\}$; F_{ρ_i}, G_{e_i}, P_i, H_{ρ_i}, H_{e_i}, R_i are matrices of suitable dimension to be computed. Denoting

$\hat{\chi}_i = \text{col}\{\chi_i,\ \rho_i\}$ and $\hat{\chi}_{e,i} = \text{col}\{\chi_{e,i},\ 0\}$, for all $t_{k_i} \in \Delta_i$ and $t_{k_i^M} \in \Delta_M$, each $i \in \mathcal{I}_0^N$ is governed by

$$\hat{\chi}_i(t_{k_i+1}) = \hat{F}_i\hat{\chi}_i(t_{k_i}) + G_i\psi_{i-1}(t_{k_i^M}) + Ef_i(t_{k_i}) - \hat{H}_i\hat{\chi}_{e,i} \tag{17}$$

with $E = \text{col}\{0,1,0,0\}$, $\hat{H}_i = \text{col}\{B_iH_{e_i},\ G_{e_i}\}$

$$\hat{F}_i = \begin{bmatrix} A_i + B_iH_{e_i} & B_i(H_{\rho_i} + H_{e_i}Q_i) \\ G_{e_i} & F_{\rho_i} \end{bmatrix}, \quad G_i = \begin{bmatrix} B_iR_i \\ P_i \end{bmatrix}.$$

In this sense, before formulating the problem, the following definitions are given.

Definition 1 (String Stability): For all $i \in \mathcal{I}_0^N$, the equilibrium $\hat{\chi}_{e,i} = \text{col}\{\chi_{e,i}, 0\}$ of (17) with $d_i \equiv 0$ is said:

(*i*) *string stable* if, for all $\varepsilon > 0$ there exists $\delta > 0$ such that for all $N \in \mathbb{N}$, $t_k \in \cup_{i=0}^N \Delta_i$

$$\max_{i\in\mathcal{I}_0^N} |\hat{\chi}_i(0) - \hat{\chi}_{e,i}| < \delta \Rightarrow \max_{i\in\mathcal{I}_0^N} |\hat{\chi}_i(t_k) - \hat{\chi}_{e,i}| < \varepsilon; \tag{18}$$

(*ii*) *asymptotically string stable* if it is string stable and for all $N \in \mathbb{N}$, $t_k \in \cup_{i=0}^N \Delta_i$

$$\lim_{t_k\to\infty} |\hat{\chi}_i(t_k) - \hat{\chi}_{e,i}| = 0. \tag{19}$$

Definition 2 (Disturbance String Stability): For all $i \in \mathcal{I}_0^N$, the equilibrium $\hat{\chi}_{e,i} = \text{col}\{\chi_{e,i}, 0\}$ of (17) is said to be *disturbance string stable* if there exist functions β_d of class $\mathcal{KL}$, σ_d of class $\mathcal{K}_\infty$ and constants $\delta > 0$ and $\delta_d > 0$ such that, for all initial conditions $\hat{\chi}_i(0) \in \mathbb{R}^{2+n_\rho}$ and disturbances $\tilde{d}_i$ satisfying

$$\max_{i\in\mathcal{I}_0^N} |\hat{\chi}_i(0) - \hat{\chi}_{e,i}| < \delta, \quad \max_{i\in\mathcal{I}_0^N} \|\tilde{d}_i\|^{[0,t_{k_i}]} < \delta_d \tag{20}$$

then, for all $N \in \mathbb{N}$, $t_k \in \cup_{i=0}^N \Delta_i$

$$\begin{aligned}\max_{i\in\mathcal{I}_0^N} |\hat{\chi}_i(t_k) - \hat{\chi}_{e,i}| \leq & \beta_d(\max_{i\in\mathcal{I}_0^N} |\hat{\chi}_i(0) - \hat{\chi}_{e,i}|, t_k) \\ & + \sigma_d(\max_{i\in\mathcal{I}_0^N} \|\tilde{d}_i\|^{[0,t_k]}).\end{aligned}$$

Problem 1: Consider a platoon of vehicles described by (4) under Assumptions 1 and 2 with the macroscopic information (13) verifying (14). Let the corresponding sampled-data microscopic model be described by (9). Design a feedback law of the form (16) so that the equilibrium $\hat{\chi}_{e,i} = \text{col}\{\chi_{e,i}, 0\}$ of (17) is disturbance string stable. □

Remark 7: It is worth to highlight that assuming the sampling sequence associated with each vehicle uniform allows the design of a time-invariant controller of the form (16) that solves Problem 1. Then, robustness can be analyzed for the closed-loop system under the so-designed control law with respect to non-uniform sampling sequences (see [26] for further details).

III. Control Design

A. Main result

Introducing the coordinate transformation $\zeta_i = \text{col}\{\chi_i - \chi_{e,i},\ \rho_i\}$ the closed-loop dynamics (17) gets the form

$$\zeta_i(t_{k_i+1}) = F_i\zeta_i(t_{k_i}) + G_i\psi_{i-1}(t_{k_i^M}) + Ef_i(t_{k_i}) \tag{21}$$

with $E = \text{col}\{0,1,0,0\}$

$$F_i = \begin{bmatrix} A_i + B_iH_{e_i} & B_i\big(H_{\rho_i} + H_{e_i}Q_i\big) \\ G_{e_i} & F_{\rho_i} + G_{e_i}Q_i \end{bmatrix}, \quad G_i = \begin{bmatrix} B_iP_i \\ R_i \end{bmatrix}.$$

At this point, the main result can be stated with the proof reported in Appendix.

Theorem 1: Problem 1 is solved by the control (16) with

$$H_{\rho_i} = -H_{e_i}Q_i \tag{22}$$

and F_{ρ_i}, G_{e_i}, P_i, H_{ρ_i}, H_{e_i}, R_i fixed so that the following conditions hold:

1) the matrices $A_i + B_iH_{e_i}$ and $F_{\rho_i} + G_{e_i}Q_i$ are Schur stable with all eigenvalues with positive real part, i.e., if $\alpha_i \in \sigma\{F_i\}$ then it gets the form $\alpha_i = e^{-\lambda_iT_i}$ for some $\lambda_i \in \mathbb{C}$ such that $\text{Re}\{\lambda_i\} > 0$;
2) the parameter

$$\gamma = \max_{i\in\mathcal{I}_0^N}\{\gamma_i(\kappa_i, r_i, g_i)\} \tag{23}$$

verifies $\gamma \in (0,1)$ with $T_{\max} = \max_{i\in\mathcal{I}_0^N}\{T_i\}$, $T_{\min} = \min_{i\in\mathcal{I}_0^N}\{T_i\}$ and $\tilde{T} = (\frac{T_{\max}}{T_{\min}} - 1)T_{\max}$, $\hat{T} = \frac{1}{T_{\min}}(T_{\max}^2 - T_{\min}^2)$, $\kappa > 0$ as in (14) and

$$\begin{aligned}
&\gamma_i(\kappa_i, r_i, g_i) = (1-\alpha_i)^{-1}\sum_{\ell=0}^{i-1}\Big(h_{i-1}^\ell p_u + \kappa g_i\bar{a}_{i-1}^\ell\Big)\beta_\ell \\
&\alpha_i = \max_{\alpha\in\sigma\{F_i\}}\{|\alpha|\},\ \beta_i = \alpha_i^{-1}|F_i|,\ g_i = |G_i|,\ r_i = |R_i| \\
&h_i^\ell = \begin{cases}\sigma_i^{\ell+1}h_\ell^\ell + \kappa\varsigma_i^{\ell+1}a_{i-1}^\ell, & \ell \in \{0,\dots,i-1\} \\ |[H_{e_i}\ H_{e_i}Q_i + H_{\rho_i}]|, & \ell = i\end{cases} \\
&a_i^\ell = \begin{cases}\sigma_i^\ell h_\ell^\ell + \kappa\varsigma_i^{\ell+1}a_\ell^\ell, & \ell \in \{0,\dots,i-1\} \\ a + \bar{p}_u h_i^i, & \ell = i\end{cases} \\
&\sigma_i^\ell = \begin{cases}\sigma_i^{\ell+1} + \bar{p}_u\kappa\varsigma_i^\ell, & \ell \in \{0,\dots,i-1\} \\ 1, & \ell = i\end{cases} \\
&\varsigma_i^\ell = \begin{cases}r_\ell\sigma_i^\ell + \varsigma_i^{\ell+1}, & \ell \in \{0,\dots,i-1\} \\ r_i, & \ell = i\end{cases} \\
&\bar{a}_i^\ell = a_\ell^\ell + \cdots + a_{i-1}^\ell,\ a = \frac{\sqrt{2}}{2}\sqrt{\hat{T}\sqrt{\hat{T}^2+4} + \hat{T}^2 + 2} \\
&p_u = \tilde{T}\sqrt{4+\tilde{T}^2}, \quad \bar{p}_u = \frac{\hat{T}}{2}\sqrt{4+\hat{T}^2}.
\end{aligned} \tag{24}$$

Remark 8: The parameter γ is contingent upon both the desired regulatory rate, which is dictated by α_i, and the significance attributed to macroscopic information, intrinsic in κg_i, associated with each vehicle. Specifically, the impact of the microscopic and macroscopic information can be regulated by properly selecting the parameters related to SS, convergence rate, and smooth behavior. For example, if there is a preference for magnifying the influence of macro information on all vehicles (i.e., $\kappa g_i \gg 0$), then α_i should approach one, resulting in a slower convergence rate and, consequently, less emphasis on micro information. Conversely, a preference for more reactive behavior with respect to microscopic information implies $\alpha_i \to 0$ and a small κg_i.

Remark 9: When all vehicles are synchronous (i.e., $T_i = T$ for all $i \in \mathcal{I}_0^N$) then $\bar{p}_u = p_u = 0$. Accordingly, the control laws (16) are identical for each vehicle; that is, one can fix $H_{e_i} = H_e$, $H_{\rho_i} = H_\rho$, $Q_i = Q$, $P_i = P$, $G_{e_i} = G_e$, $F_{\rho_i} = F_\rho$ and $R_i = R$ for all $i \in \mathcal{I}_0^N$ so getting $\bar{a}_{i-1}^{\ell} = 1$ for all $\ell \in \mathcal{I}_0^N$. In that case, the parameter γ in (23) reads

$$\gamma = \kappa\beta g(1 - e^{-\lambda_{\min} T})^{-1}, \quad \lambda_{\min} > 0. \tag{25}$$

This highlights that, for a fixed $\lambda_{\min} > 0$, if the sampling period is large then the macro information must be given a small weight so that the micro information is favored. Indeed, in this case, the macro information brings a poor contribution due to the large microscopic sampling. On the other side, if sampling is fast ($\lambda_{\min} \to 0$), the macro information is richer in contribution, and κg can be set larger.

Remark 10: The form (25) highlights that the results can be interpreted as a sensitivity analysis of the control systems with respect to variations in the sampling period. For a fixed choice of the parameters of the control law (16), the problem is solved for all sampling periods verifying $\gamma \in (0, 1)$. Accordingly, one can deduce from (25) an upper bound on T estimating the maximum allowed sampling period still guaranteeing that Problem 1 is solved. With due complications, the same holds for the general case of (23) which, for a fixed choice of the controller (16), allows to estimate the maximum allowed involved sampling period $T_{\max}$ guaranteeing that the problem is solved.

Remark 11: As shown in the next section, when either the spacing policy is constant or it only involves the microscopic information, a static mesoscopic control law can be used. However, in general, a dynamical component of the form (16) might be necessary. This is because, in general, $\rho_{\mathtt{m},i}(t_{k_i+1})$ is not directly available to each vehicle $i \in \mathcal{I}_0^N$ as it would require an explicit prediction of the macroscopic information (13).

Remark 12: In general, the dimension and definition of the dynamic component in (16) can vary depending on the kind of macro information at hand and possible further requirements to be accomplished. A general choice, however, might be obtained setting $G_{e_i} = 0$, $P_i = 0$, and F_{ρ_i} any Schur matrix. In that case, the dimension depends however on the particular form of the mesoscopic spacing policy (15) and of the macroscopic function (13).

Next, a particular spacing policy for which static feedback can be computed is presented.

B. Constant spacing policy

In this section, we are specifying the result by Theorem 1 when the spacing policy (15) is of the form $\rho_{\mathtt{m},i} := 0$. In this case, the controller (16) reduces to the static feedback

$$u_i(t_{k_i}) = u_{i-1}(t_{k_i}) + H_{e_i} e_i(t_{k_i}) + P_i \psi_{i-1}(t_{k_i^M}) \tag{26}$$

with, hence, $e_i = \chi_i - \chi_{e,i}$, $F_{\rho_i} = H_{\rho_i} = G_{e_i} = R_i = 0$, for all $i \in \mathcal{I}_0^N$. While the spacing policy does not directly incorporate macroscopic information, its influence is reflected in the controllers. Consequently, the control law maintains a mesoscopic character.

In that case, a static controller of the form (16) with $n_\rho = 0$ is constructed in the next result, which is a corollary of Theorem 1.

Corollary 1: When the spacing policy (15) is constant (i.e., $\rho_{\mathtt{m},i} \equiv 0$ for all $i \in \mathcal{I}_0^N$), the feedback (26) solves Problem 1 provided that the following conditions hold:

1) the matrix $A_i + B_i H_{e_i}$ is Schur stable with all eigenvalues with positive real part, i.e., if $\alpha_i \in \sigma\{A_i + B_i H_{e_i}\}$ then it gets the form $\alpha_i = e^{-\lambda_i T_i}$ for some $\lambda_i \in \mathbb{C}$ such that $\mathrm{Re}\{\lambda_i\} > 0$;
2) the parameter (23) verifies $\gamma \in (0, 1)$ with $\kappa > 0$ in (14) and (24) specifying as

$$\alpha_i = \max_{\alpha \in \sigma\{A_i + B_i H_{e_i}\}} \{|\alpha|\}, \quad \beta_i = \alpha_i^{-1} |F_i|$$
$$g_i = \frac{T_i}{2} \sqrt{4 + T_i^2} r_i, \quad r_i = |R_i|.$$

The result above highlights an explicit dependency of the parameter γ in (23) on the sampling period. In particular, the larger the sampling period, the smaller the corresponding term γ_i via the choice of the parameters $r_i > 0$ (weighting the effect of the macro-information) and α_i (weighting the convergence rate to the desired equilibrium).

C. A class of mesoscopic spacing policies

We fix now the spacing policy (15) as

$$\rho_{\mathtt{m},i}(t_{k_i}) := -C \tilde{\psi}_{i-1}(t_{k_i}) \tag{27}$$

with

$$\tilde{\psi}_{i-1}(t_{k_i}) = \begin{cases} \psi_{i-1}(t_{k_i - 1}), & \text{if } t_{k_i} \notin \Delta_i^M \\ \psi_{i-1}(t_{k_i}^M), & \text{otherwise} \end{cases} \tag{28}$$

and $C \in \mathbb{R}^{1 \times 2}$ a suitable matrix so getting $e_i = \chi_i - \chi_{e,i} + \bar{C} \tilde{\psi}_{i-1}(t_{k_i})$ with $\bar{C} = \mathrm{col}\{C, 0\}$. In contrast to the constant spacing policy detailed in Section III-B, in this case, macroscopic information directly shapes the spacing policy, thereby influencing the trajectory to be tracked. For this reason, we name the policy as mesoscopic spacing policy. The impact of the macroscopic information is expected to settle the targeted gap with respect to real-time traffic conditions. In this case, the problem is solved by a feedback of the form (16) with $n_\rho = 1$ as further specified below.

Proposition 1: When the spacing policy (15) is with $\rho_{\mathtt{m},i}$ as in (27) for all $i \in \mathcal{I}_0^N$, the feedback (16) with $\rho_i \in \mathbb{R}$,

$$F_{\rho_i} = e^{-\lambda_{\rho_i} T_i}, \quad G_{e_i} = 0, \quad R_i = 0, \quad Q_i = 1 \tag{29}$$

$\lambda_{\rho_i} > 0$, H_{ρ_i} in (22) solves Problem 1 provided that the following conditions hold:

1) the matrix $A_i + B_i H_{e_i}$ is Schur stable with all eigenvalues with positive real part, i.e., if $\alpha_i \in \sigma\{A_i + B_i H_{e_i}\}$ then it gets the form $\alpha_i = e^{-\lambda_i T_i}$ for some $\lambda_i \in \mathbb{C}$ such that $\mathrm{Re}\{\lambda_i\} > 0$;

2) the parameter (23) verifies $\gamma \in (0,1)$ with $\kappa > 0$ in (14) and (24) specifying with

$$\alpha_i = \max_{\alpha \in \sigma\{F_i\}} \{|\alpha|\},\ \beta_i = |F_i|{\alpha_i}^{-1},\ g_i = |P_i|,\ r_i = 0.$$

Proof: The proof follows from Theorem 1. It is worth seeing that, an alternative is obtained via the transformation

$$\bar{\zeta}_i(t_{k_i}) = \zeta_i(t_{k_i}) + \bar{C}\tilde{\psi}_{i-1}(t_{k_i}) \tag{30}$$

with $\bar{C} = \text{col}\{C, 0\} \in \mathbb{R}^{3\times 2}$, setting $Q_i\rho_i = \text{col}\{C\tilde{\psi}_{i-1}(t_{k_i}), 0\}$ for $Q_i = \text{col}\{1, 0\}$. In those coordinates, the closed-loop (21) reads

$$\bar{\zeta}_i(t_{k_i+1}) = \bar{F}_i\bar{\zeta}_i(t_{k_i}) + E_i f_{T_i}(d_{i,t_{k_i}})$$
$$\bar{F}_i = \begin{bmatrix} A_i + B_iH_{e_i} & Q_iF_{\rho_i} - \big(A_i + B_i(H_{e_i} - R_iC^\dagger)\big)Q_i \\ 0 & e^{-\lambda_{\rho_i}T_i} \end{bmatrix}.$$

Thus, exponential stability of all $i \in \mathcal{I}_0^N$ follows as well as Input-to-State Stability (ISS). At this point, SS can be directly inferred from the definition of (30) and the exponential stability of the closed loop. ■

Remark 13: In this case, we include the macroscopic function (13), evaluated at $t = t_{k_i}^M$ with $t_{k_i}^M \in \Delta_i^M$, in the spacing policy to track (15). Thus, a dynamic controller of dimension one is employed to solve Problem 1. Current work is toward the definition of further components of the controller to reconstruct the macroscopic function (13) at all other sampling instants based on distributed prediction to improve the performances of the closed-loop platoon.

IV. Simulations

The proposed sampled-data control strategy is here verified in simulation in MATLAB under realistic settings. We consider a platoon of $N = 9$ vehicles. The constant reference distance is $\Delta\bar{p} = 20$ m and the initial desired speed of the leading vehicle is $\bar{v} = 20$ m/s. The vehicle speed is such that $0 \le v_i \le 36$ m/s, and the acceleration is bounded by $-7 \le u_i \le 7$ m/s^2. The seventh and eighth vehicles (i.e., $i = 7$ and $i = 8$) have initial distances equal to 18 m and 22 m respectively, whereas all others have initial distances at the equilibrium equal to one, i.e., $\Delta\bar{p}$. All vehicles are initialized with the same initial speed at $t = t_0 = 0$ that corresponds to the desired one associated with the primer vehicle. The simulation time is 60 s. the leader of the platoon tracks a piecewise constant reference speed profile $v_{ref}(t)$ (Fig. 1) that is split as follows: 1) for $t \in [0, 20)$ s, $v_{ref} = 20$ m/s; 2) for $t \in [20, 30)$ s, $v_{ref} = 22$ m/s; 3) for $t \in [30, 40)$ s, $v_{ref} = 20$ m/s; 4) for $t \in [40, 50)$ s, $v_{ref} = 18$ m/s; 5) for $t \in [50, 60]$ s, $v_{ref} = 20$ m/s.

Considering the disturbances affecting the vehicles, the simulation time is divided into distinct phases: 1) for $t \in [0, 10) \cup [15, 20) \cup [25, 40) \cup [50, 60]$, no disturbance is acting over, i.e., $d_i \equiv$ for all $i \in \mathcal{I}_0^9$; 2) for $t \in [10, 15)$ s, a constant disturbance $d_1 = 3$ acts on the first vehicle vehicle only; 3) for $t \in [20, 25)$ s, a constant disturbance $d_1 = -3$ acts on the $i = 1$ vehicle; 4) for $t \in [40, 50)$ s, a sinusoidal disturbance is acting on each vehicle of the platoon.

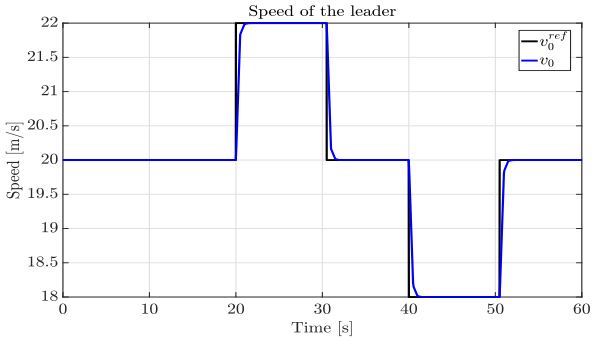

Fig. 1: Speed of the platoon leader and its reference.

By leveraging the relationship among macroscopic density and microscopic variance as introduced in [42], similarly to [12], we consider the following macroscopic function $\psi_{i-1}(t_{k_i^M})$ for (13)

$$\psi_{i-1}(t_{k_i^M}) = \text{col}\{\psi_{i-1}^{\Delta p}(t_{k_i^M}),\ \psi_{i-1}^{\Delta v}(t_{k_i^M})\}, \tag{31}$$

where, for $\bar{\Delta} \in \{\Delta p, \Delta v\}$,

$$\psi_{i-1}^{\Delta p}(t_{k_i^M}) = \text{sign}(\Delta\bar{p} + \mu_{\Delta p,i-1}(t_{k_i^M}))\sqrt{\sigma^2_{\Delta p,i-1}(t_{k_i^M})},$$
$$\psi_{i-1}^{\Delta v}(t_{k_i^M}) = \text{sign}(\mu_{\Delta v,i-1}(t_{k_i^M}))\sqrt{\sigma^2_{\Delta v,i-1}(t_{k_i^M})}$$
$$\mu_{\bar{\Delta},i-1}(t_{k_i^M}) = \frac{1}{i}\sum_{j=1}^{i}\bar{\Delta}_j(t_{k_i^M})$$
$$\sigma^2_{\bar{\Delta},i-1}(t_{k_i^M}) = \frac{1}{i}\sum_{j=1}^{i}(\bar{\Delta}_j(t_{k_i^M}) - \mu_{\bar{\Delta}_i}(t_{k_i^M}))^2.$$

We evaluate the performance of the developed sampled-data controllers in two main scenarios: (Case 1) the entire fleet synchronously updates microscopic and macroscopic information, that is, $T = T_i = 0.5$ s for all $i \in \mathcal{I}_0^N$ and $T^M = T_i^M = 3$ s, i.e., $m = 6$; (Case 2) the updates are fully asynchronous, i.e., we consider the sampling periods T_i reported in Table I, as randomly generated with a small variance and an average equal to 0.1066 s. As far as the macroscopic information is concerned, we consider updates on macroscopic information to take place by fixing $m = 5$ in the asynchronous scenario. The choice of the larger sampling time for the synchronous case has been made as a comparison of similar sampling period would not be fair.

Lastly, as a third scenario (Case 3), we consider an asynchronous platoon where the macroscopic information is not tailored for each vehicle but is taken equally for all of them. It represents a disturbance acting on the macroscopic information. Clearly, the higher the difference between the tailored macroscopic information and the considered one, the larger the disturbance. Moreover, to better remark on the robustness with respect to this kind of perturbation, the macroscopic sampling periods are set according to $m = 46$. In the latter case, we stress that even if the macro information is synchronously shared through the platoon (see the third plots in Fig. 6 and 7), each vehicle accesses it at distinct time instants $t_{k_i^M} \in \Delta_i^M$. This implies that if T_i^M is small, the corresponding vehicle

might access the same information multiple times whereas, on the other side, if T_i^M is large, packet losses might occur.

The color legends are consistent across all figures. Each line in the figure corresponds to the trajectory of the leader-follower variable specific to that figure. The color gradient, transitioning from a blue tint to a light green shade, represents the sequence of vehicles in the platoon, ranging from the lead vehicles to the trailing ones.

A. Case 1: Synchronous sampling

In this analysis, we explore the SS of the platoon using the mesoscopic spacing policy defined in (15) and (27). The investigation is conducted under synchronous sampling, where each vehicle receives tailored macroscopic information. It is important to note the microscopic sampling interval is $T = T_i = 0.5$ s (Assumption 1) whereas the macroscopic one is fixed to $T^M = T_i^M = 3$ s (Assumption 2) for all vehicles with $m = 6$.

The synchronous scenario experiences a notable impact due to the relatively low sampling rates for both microscopic and macroscopic information. The resulting γ value is 0.10852, meeting the conditions outlined in Theorem 1. Fig. 2 illustrates the dynamic evolution of distances, speed differentials, macroscopic information, and control inputs for the mesoscopic spacing policy. Particularly, the first and second plots in Fig. 2 portray distances and speed differentials within the platoon, showcasing evident SS since the error of distances and differences of speeds reduces along the platoon (see also Fig. 3). Notably, during the time interval $t = 0$ s to $t = 10$ s, when no disturbances act on the system, the trailing vehicle responds to variations in distances from its predecessors due to distinct initial conditions. It adeptly utilizes macroscopic information to fine-tune its distance and speed accordingly. The third plot in Fig. 2 presents the linear combination of macroscopic function components in (31), while the last one displays the control inputs. Subsequently, beyond $t = 10$ s, the effect of disturbances is attenuated along the platoon, as evident from the first and second plots in Fig. 2 (as well as in the zoom in Fig. 3). Despite the slow sampling rate, the entire set of vehicles does not perfectly reject the dynamics impacted by fast disturbances. Nevertheless, as proved in Theorem 1, the system response remains (disturbance) string stable, with distance and speed errors decreasing in magnitude as the number of vehicles increases.

B. Case 2: Asynchronous sampling

In a manner akin to the preceding scenario, we delve into the investigation of SS within the platoon, employing the mesoscopic spacing policy. However, in contrast, we explore asynchronous sampling among the vehicles, as well as between the microscopic and macroscopic rates. The microscopic sampling rate for each vehicle is detailed in Table I, with the macroscopic sampling sequence yielded setting $m = 5$ (Assumption 2). Alongside the other selected parameters, this configuration yields $\gamma = 0.85921$, fulfilling the condition stipulated in Theorem 1. As in the synchronous case, we introduce Fig. 4 to visually depict the dynamic evolution of distances, speed differentials, macroscopic information, and control inputs.

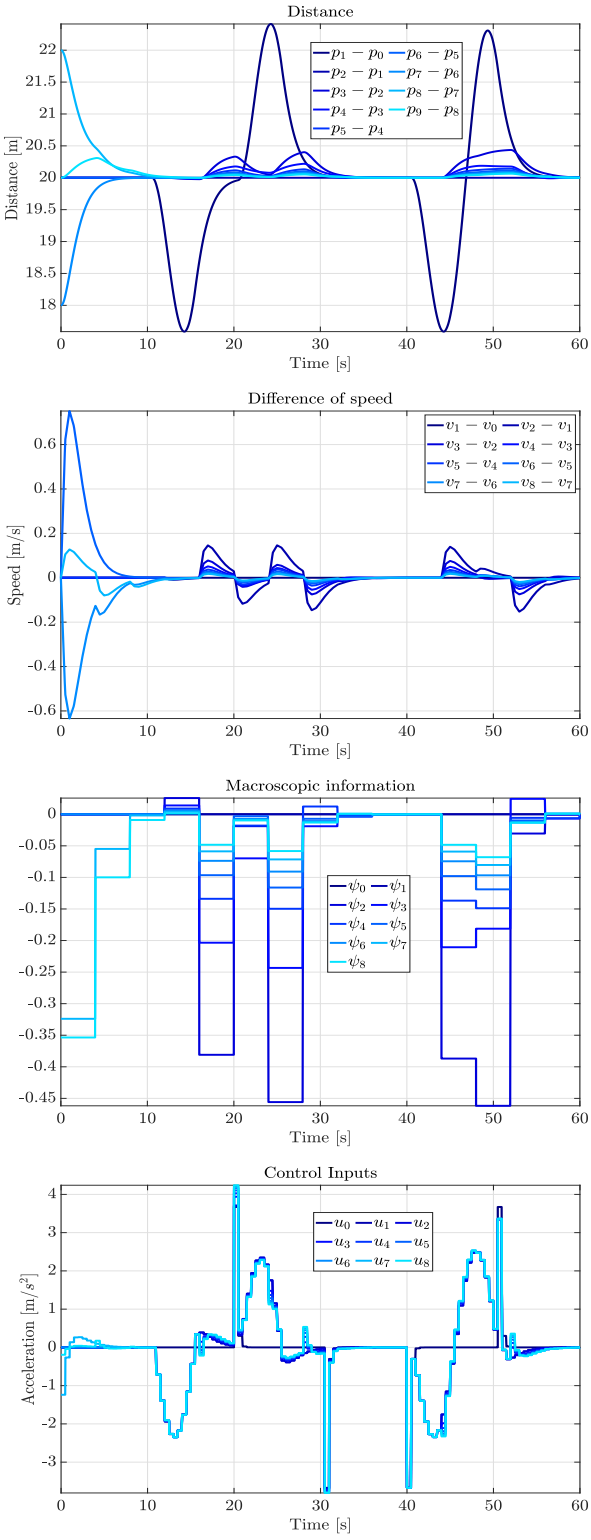

Fig. 2: Case 1 in case of mesoscopic spacing policies. See Section IV for the description and the color legend.

Due to the dual challenges posed by stringent requirements for faster and asynchronous sampling, a noticeable distinction emerges upon comparing Fig. 4 with Fig. 2.

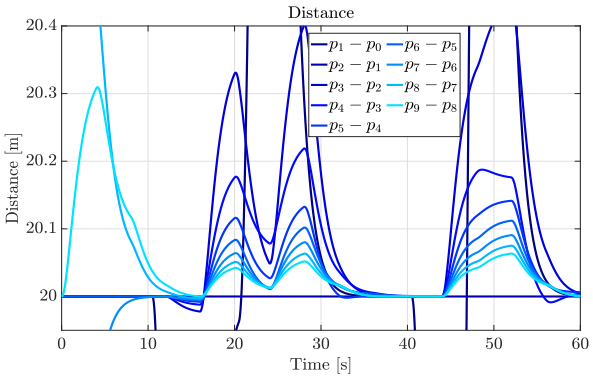

Fig. 3: Zoom of the distance displacement in Fig. 2

Notably, the controllers in Fig. 4 exhibit increased solicitation in this scenario, reaching saturation multiple times. The asynchronous sampling significantly impacts the system's performance. Nevertheless, the characteristic of SS remains intact.

As depicted in the first two plots of Fig. 4 (and in the corresponding zoom in Fig. 5), the error does not propagate along the platoon. The last vehicle exhibits superior behavior almost throughout, with a minor setback around $t = 40$ s. As $t \in (40.5, 41.5)$ s, the last vehicle experiences a downturn in both distance and speed performance. This deviation results from the unfortunate alignment of the fast variation in the reference for the leader vehicle (that we impose on purpose), necessitating a trajectory variation for the entire platoon. The macroscopic sampling at the last vehicle occurs too late in response to the platoon's trajectory change. This delay contributes to the observed overshoot, as illustrated in the corresponding plots in Fig. 4. It is noteworthy that the last vehicle still counters this deviation, ceasing the propagation of perturbations after approximately one second. This manifestation underscores the robustness of the proposed approach.

T_1	T_2	T_3	T_4	T_5
0.1097	0.1096	0.1049	0.1080	0.1014
T_6	T_7	T_8	T_9	
0.1042	0.1092	0.1079	0.1096	

TABLE I: Values of T_i for $i \in \{1, \dots, 9\}$ in Cases 2 and 3.

C. Case 3: Asynchronous sampling with disturbance

In the realm of vehicle i, when the bespoke information ψ_i in (13) either encounters imperfections or is subject to disturbances, the summation of signals can be construed as an average quantity. This quantity represents macroscopic information, devoid of specific computation concerning the leading vehicles of i. It considers the ideal neighborhood, furnishing the most effective information for attaining SS. To elucidate the controllers' response to disturbances affecting macroscopic information, we evaluate each vehicle using the function ψ_N instead of the tailored ψ_{i-1}. To illustrate the impact of a disturbance on macroscopic information, we compare constant and mesoscopic spacing policies (refer to Fig. 6 for constant and 7 for mesoscopic).

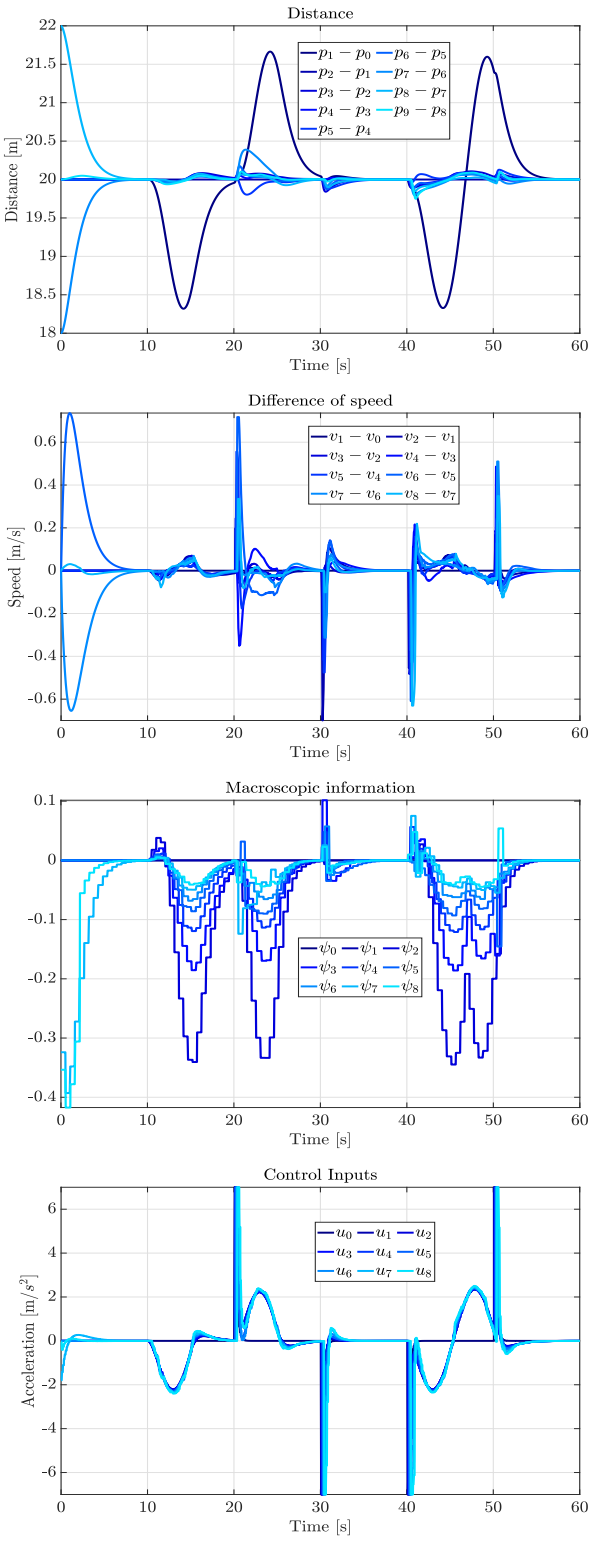

Fig. 4: Case 2 in case of mesoscopic spacing policies.

The microscopic sampling aligns with that of Case 2 (refer to Table I), while the macroscopic sampling is increased to better discern differences between spacing policies, yielded by the choice of $m = 46$. The third plots in Fig. 6 and 7 depict the macroscopic information ψ, computed based on the last vehicle but transmitted to the entire set of vehicles. This case yields $\gamma = 0.85921$. The time interval

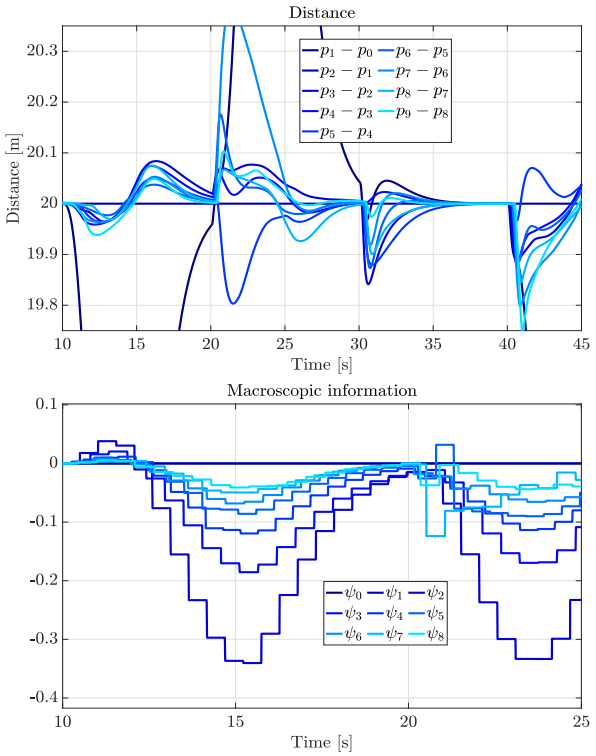

Fig. 5: Zoom of distance displacement and the macroscopic information in Fig. 4

delineated by $t \in [0, 10)$ s provides a clearer understanding of the distinctions between the spacing policies. The first two plots in Fig. 7 illustrate that the platoon dynamics employing the mesoscopic spacing policy are more influenced than those under the constant policy, depicted in Fig. 6. While both cases grapple with non-tailored macroscopic information, the constant spacing policy is less affected, as expected. Despite sharing the critical point around $t = 40$ s with the simulations in Case 2, they demonstrate the ability to achieve DSS throughout the entire simulation. Clearly, the two spacing policies manifest distinct characteristics. The constant policy facilitates smoother dynamics, with its microscopic equilibrium being less affected by macroscopic information. Conversely, the mesoscopic policy allows for a higher anticipatory response, resulting in shorter transients as shown in the second plot in Fig. 7.

The simulations show the capability of the suggested methodology to ensure DSS under synchronous or asynchronous sampling for a platoon of heterogeneous vehicles.

V. Conclusions

The present paper introduces a sampled-data mesoscopic controller designed to ensure disturbance string stability in a platoon of heterogeneous vehicles with non-uniform sampling rates. The design is not only constructive but also provides easily verifiable conditions to attain optimal performance and safety. Furthermore, the paper includes a detailed discussion on how to effectively balance performance and safety according to specific needs.

Future research emphasizes the development of distributed prediction algorithms for macroscopic information and the adaptation of a broader range of spacing policies to the proposed approach. This would improve performance and reduce the impact of unfortunate sampling with respect to fast variations. Extensions involving packet losses, quantization, and transmission delays are foreseen.

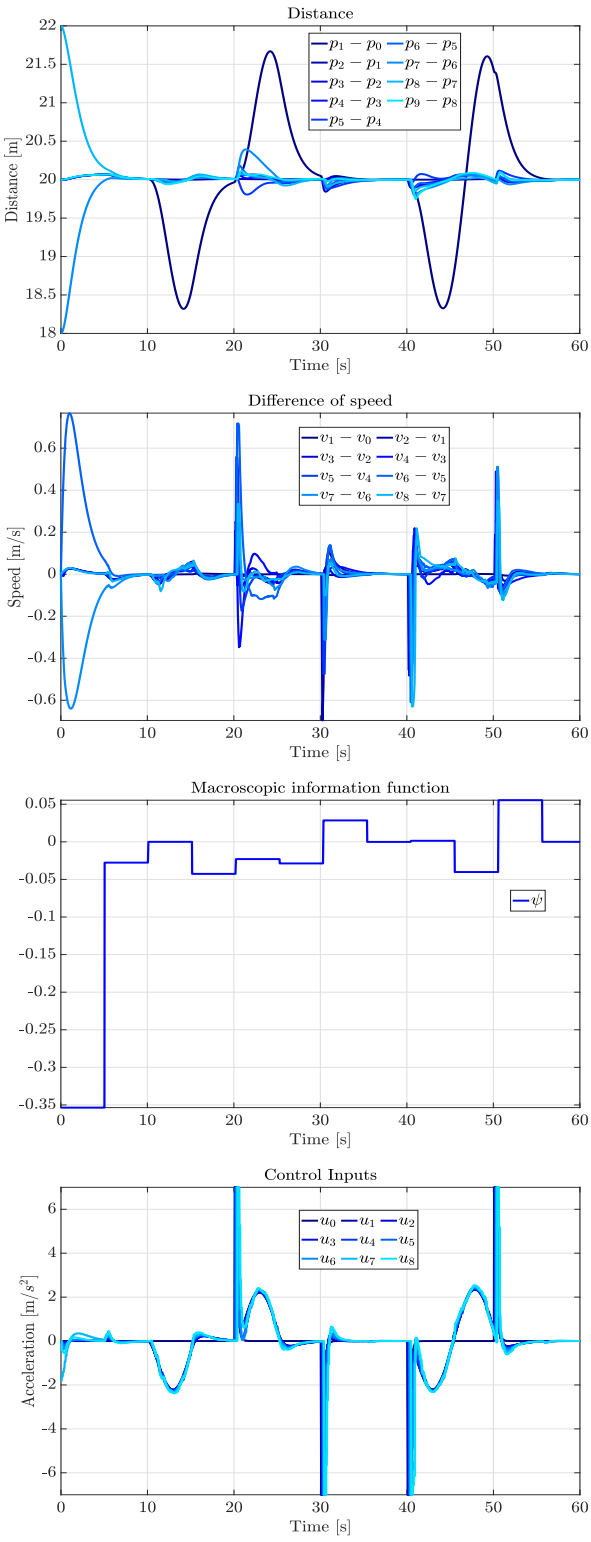

Fig. 6: Case 3 in case of constant spacing policies.

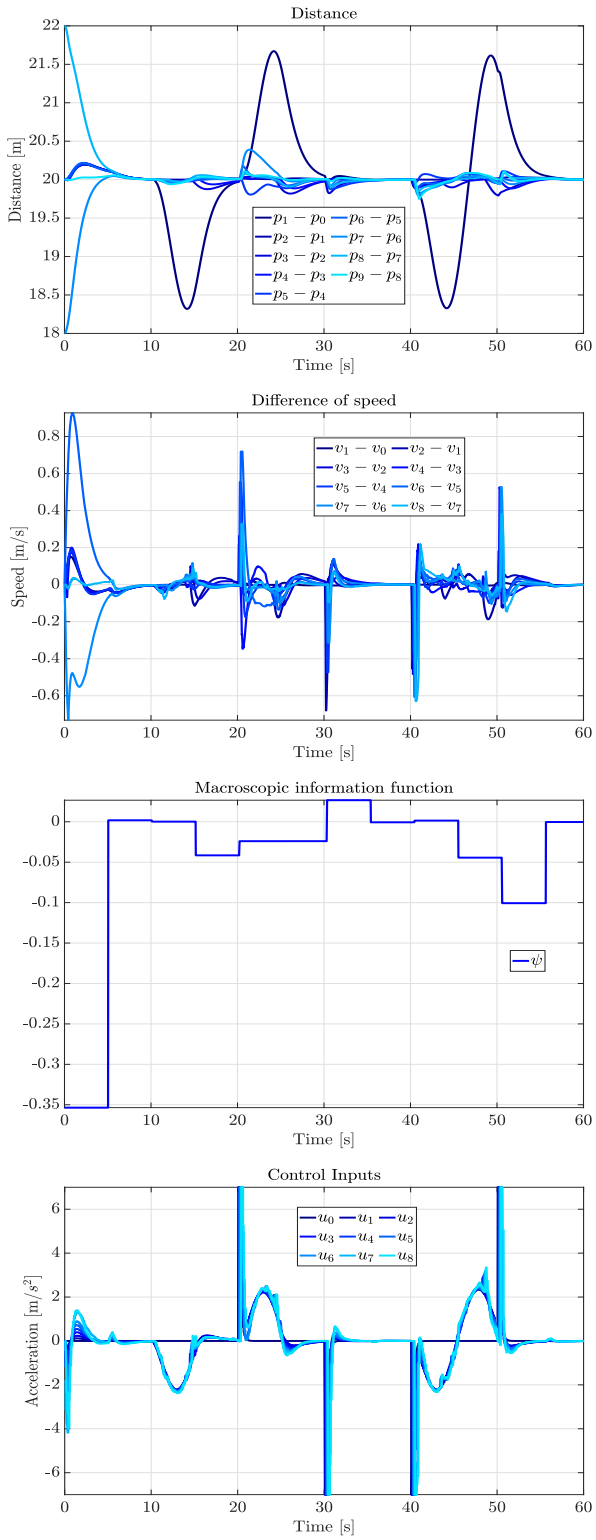

Fig. 7: Case 3 in case of mesoscopic spacing policies.

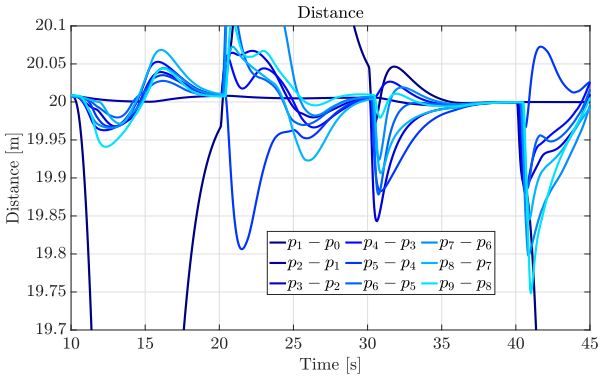

Fig. 8: Zoom of distance displacement in Fig. 6

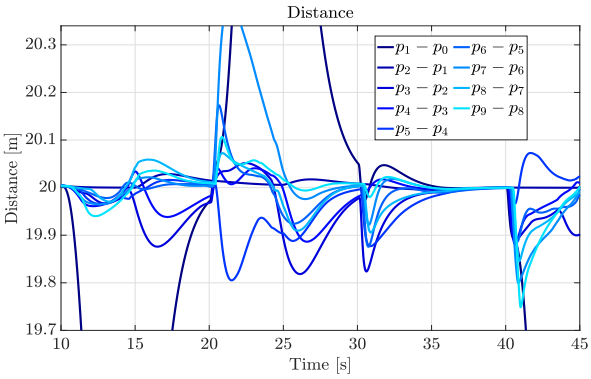

Fig. 9: Zoom of distance displacement in Fig. 7

References

[1] J. Guanetti, Y. Kim, and F. Borrelli, "Control of connected and automated vehicles: State of the art and future challenges," *Annual Reviews in Control*, vol. 45, pp. 18–40, 2018.

[2] R. E. Stern, S. Cui, M. L. Delle Monache, R. Bhadani, M. Bunting, M. Churchill, N. Hamilton, R. Haulcy, H. Pohlmann, F. Wu, B. Piccoli, B. Seibold, J. Sprinkle, and D. B. Work, "Dissipation of stop-and-go waves via control of autonomous vehicles: Field experiments," *Transportation Research Part C: Emerging Technologies*, vol. 89, 2018.

[3] S. Feng, Y. Zhang, S. E. Li, Z. Cao, H. X. Liu, and L. Li, "String stability for vehicular platoon control: Definitions and analysis methods," *Annual Reviews in Control*, vol. 47, pp. 81–97, March 2019.

[4] P. Nilsson, O. Hussien, A. Balkan, Y. Chen, A. D. Ames, J. W. Grizzle, N. Ozay, H. Peng, and P. Tabuada, "Correct-by-construction adaptive cruise control: Two approaches," *IEEE Transactions on Control Systems Technology*, vol. 24, no. 4, pp. 1294–1307, 2016.

[5] F. Liberati, A. D. Giorgio, and G. Koch, "Optimal stochastic control of energy storage system based on pontryagin minimum principle for flattening pev fast charging in a service area," *IEEE Control Systems Letters*, vol. 6, pp. 247–252, 2022.

[6] D. Swaroop and J. K. Hedrick, "String stability of interconnected systems," *IEEE Transactions on Automatic Control*, vol. 41, no. 3, pp. 349–357, Mar 1996.

[7] J. Monteil, M. Bouroche, and D. J. Leith, "$\mathcal{L}_2$ and $\mathcal{L}_\infty$ stability analysis of heterogeneous traffic with application to parameter optimization for the control of automated vehicles," *IEEE Transactions on Control Systems Technology*, vol. 27, no. 3, pp. 934–949, 2019.

[8] B. Besselink and K. H. Johansson, "String stability and a delay-based spacing policy for vehicle platoons subject to disturbances," *IEEE Transactions on Automatic Control*, vol. 62, no. 9, pp. 4376–4391, March 2017.

[9] Y. Zheng, S. E. Li, K. Li, F. Borrelli, and J. K. Hedrick, "Distributed model predictive control for heterogeneous vehicle platoons under unidirectional topologies," *IEEE Transactions on Control Systems Technology*, vol. 25, no. 3, pp. 899–910, 2017.

[10] S. Darbha, S. Konduri, and P. R. Pagilla, "Benefits of v2v communication for autonomous and connected vehicles," *IEEE Transactions on Intelligent Transportation Systems*, vol. 20, no. 5, pp. 1954–1963, 2019.

[11] E. Abolfazli, B. Besselink, and T. Charalambous, "Minimum time headway in platooning systems under the mpf topology for different wireless communication scenario," *IEEE Transactions on Intelligent Transportation Systems*, vol. 24, no. 4, 2023.

[12] M. Mirabilio, A. Iovine, E. De Santis, M. D. Di Benedetto, and G. Pola, "String stability of a vehicular platoon with the use of macroscopic information," *IEEE Transactions on Intelligent Transportation Systems*, vol. 22, no. 9, pp. 5861–5873, 2021.

[13] ——, "Mesoscopic controller for string stability of platoons with disturbances," *IEEE Transactions on Control of Network Systems*, vol. 9, no. 4, pp. 1754–1766, 2022.

[14] I. Karafyllis, D. Theodosis, and M. Papageorgiou, "Nonlinear adaptive cruise control of vehicular platoons," *International Journal of Control*, vol. 96, no. 1, pp. 147–169, 2023.

[15] D. Swaroop and R. Huandra, "Intelligent cruise control system design based on a traffic flow specification," *Vehicle System Dynamics: International Journal of Vehicle Mechanics and Mobility*, vol. 30, no. 5, pp. 319–344, November 1998.

[16] S. Darbha and K. Rajagopal, "Intelligent cruise control systems and traffic flow stability," *Transportation Research Part C: Emerging Technologies*, vol. 7, no. 6, pp. 329–352, 1999.

[17] A. Iovine, F. Valentini, E. De Santis, M. D. Di Benedetto, and M. Pratesi, "Safe human-inspired mesoscopic hybrid automaton for autonomous vehicles," *Nonlinear Analysis: Hybrid Systems*, vol. 25, pp. 192 – 210, 2017.

[18] A. Jamshidnejad, I. Papamichail, M. Papageorgiou, and B. De Schutter, "A mesoscopic integrated urban traffic flow-emission model," *Transportation Research Part C: Emerging Technologies*, vol. 75, pp. 45 – 83, 2017.

[19] A. Ibrahim, M. Čičić, D. Goswami, T. Basten, and K. Johansson, "Control of platooned vehicles in presence of traffic shock waves," *IEEE Intelligent Transportation Systems Conference*, 2019.

[20] M. Mirabilio, A. Iovine, E. De Santis, M. D. Di Benedetto, and G. Pola, "A mesoscopic human-inspired adaptive cruise control for eco-driving," *IEEE Transactions on Intelligent Transportation Systems*, vol. 24, no. 9, pp. 9571–9583, 2023.

[21] M. Delle Monache and P. Goatin, "Scalar conservation laws with moving constraints arising in traffic flow modeling: An existence result," *Journal of Differential Equations*, vol. 257, no. 11, pp. 4015–4029, 2014.

[22] M. Garavello, P. Goatin, T. Liard, and B. Piccoli, "A multiscale model for traffic regulation via autonomous vehicles," *Journal of Differential Equations*, vol. 269, no. 7, pp. 6088–6124, 2020.

[23] G. Piacentini, P. Goatin, and A. Ferrara, "A macroscopic model for platooning in highway traffic," *SIAM Journal on Applied Mathematics*, vol. 80, no. 1, pp. 639–656, 2020.

[24] S. Monaco and D. Normand-Cyrot, "Issues on nonlinear digital control," *European Journal of Control*, vol. 7, no. 2-3, pp. 160–177, 2001.

[25] J. I. Yuz and G. C. Goodwin, "On sampled-data models for nonlinear systems," *IEEE Transactions on Automatic Control*, vol. 50, no. 10, pp. 1477–1489, 2005.

[26] L. Hetel, C. Fiter, H. Omran, A. Seuret, E. Fridman, J.-P. Richard, and S. I. Niculescu, "Recent developments on the stability of systems with aperiodic sampling: An overview," *Automatica*, vol. 76, pp. 309–335, 2017.

[27] M. Mattioni, S. Monaco, and D. Normand-Cyrot, "Feedforwarding under sampling," *IEEE Transactions on Automatic Control*, vol. 64, no. 11, pp. 4668–4675, 2019.

[28] I. Karafyllis and C. Kravaris, "Global stability results for systems under sampled-data control," *International Journal of Robust and Nonlinear Control: IFAC-Affiliated Journal*, vol. 19, no. 10, pp. 1105–1128, 2009.

[29] M. Di Ferdinando and P. Pepe, "Sampled-data emulation of dynamic output feedback controllers for nonlinear time-delay systems," *Automatica*, vol. 99, pp. 120–131, 2019.

[30] D. Theodosis, F. N. Tzortzoglou, I. Karafyllis, I. Papamichail, and M. Papageorgiou, "Sampled-data controllers for autonomous vehicles on lane-free roads," in *2022 30th Mediterranean Conference on Control and Automation (MED)*, 2022.

[31] G. Guo and W. Yue, "Sampled-data cooperative adaptive cruise control of vehicles with sensor failures," *IEEE Transactions on Intelligent Transportation Systems*, 2014.

[32] A. Iovine, M. Mattioni, and G. Tedeschi, "Sampled-data string stability for a platoon of heterogeneous vehicles via a mesoscopic approach," in *2024 European Control Conference (ECC)*, 2024, pp. 3364–3369.

[33] L. Xiao and F. Gao, "Practical string stability of platoon of adaptive cruise control vehicles," *IEEE Transactions on Intelligent Transportation Systems*, vol. 12, no. 4, 2011.

[34] V. K. Vegamoor, S. Darbha, and K. R. Rajagopal, "A review of automatic vehicle following systems," *Journal of the Indian Institute of Science*, vol. 99, p. 567 – 587, 2019.

[35] M. di Bernardo, A. Salvi, and S. Santini, "Distributed consensus strategy for platooning of vehicles in the presence of time-varying heterogeneous communication delays," *IEEE Transactions on Intelligent Transportation Systems*, vol. 16, no. 1, 2015.

[36] V. Giammarino, S. Baldi, P. Frasca, and M. L. Delle Monache, "Traffic flow on a ring with a single autonomous vehicle: An interconnected stability perspective," *IEEE Transactions on Intelligent Transportation Systems*, vol. 22, no. 8, 2021.

[37] J. Ploeg, N. van de Wouw, and H. Nijmeijer, "$\mathcal{L}_p$ string stability of cascaded systems application to vehicle platooning," *IEEE Transactions on Control Systems Technology*, vol. 22, no. 2, pp. 786–793, March 2014.

[38] S. Baldi, D. Liu, V. Jain, and W. Yu, "Establishing platoons of bidirectional cooperative vehicles with engine limits and uncertain dynamics," *IEEE Transactions on Intelligent Transportation Systems*, vol. 22, no. 5, pp. 2679–2691, 2021.

[39] Y. Kim, J. Guanetti, and F. Borrelli, "Compact cooperative adaptive cruise control for energy saving: Air drag modelling and simulation," *IEEE Transactions on Vehicular Technology*, vol. 70, no. 10, pp. 9838–9848, 2021.

[40] S. Monaco and D. Normand-Cyrot, "On the sampling of a linear analytic control system," in *1985 24th IEEE Conference on Decision and Control*. IEEE, 1985, pp. 1457–1462.

[41] L. P. Njoua Dongmo, J. Auriol, and A. Iovine, "Smart traffic manager for speed harmonisation and stop-and-go waves mitigation dedicated to connected autonomous vehicles," *IEEE Transactions on Control Systems Technology*, to appear. [Online]. Available: https://hal.science/hal-04680301v1/document

[42] M. Treiber and A. Kesting, *Traffic flows dynamics*. Springer, 2013.

[43] Z.-P. Jiang and Y. Wang, "Input-to-state stability for discrete-time nonlinear systems," *Automatica*, vol. 37, no. 6, pp. 857–869, 2001.

[44] M. Mattioni, S. Monaco, and D. Normand-Cyrot, "Forwarding stabilization in discrete time," *Automatica*, vol. 109, 2019.

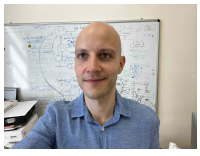

Mattia Mattioni received his PhD in Automatica from *Université Paris-Saclay* and *Università degli Studi di Roma La Sapienza* in 2018. He received the BSc and MSc in Control Engineering (both Magna cum Laude) from *La Sapienza Università di Roma* (Italy) in, respectively, 2012 and 2015. In 2015, he participated to the double-degree program *STIC&A* with *Université Paris Sud XI*. Since August 2022, he has been tenure-track assistant professor at *DIAG A. Ruberti* (*Università degli Studi di Roma La Sapienza*). His research is mainly concerned with hybrid, multi-agent and time-delay systems and stabilization of nonlinear systems via sampled-data feedback.

Alessio Iovine (M'18) received the B.Sc. and M.Sc. degrees in electrical engineering and computer science from the University of L'Aquila, L'Aquila, Italy, in 2010 and 2012, respectively, and the European Doctorate degree in information science and engineering in 2016 from the University of L'Aquila, L'Aquila, Italy, in collaboration with CentraleSupélec, Paris-Saclay University, Gif-sur-Yvette, France. In 2020, he joined the CNRS as Researcher and is with the L2S, Paris-Saclay University. Dr. Iovine has co-authored more than 50 peer-reviewed papers covering advanced control methods for power and energy systems as well as traffic control ones, with smart grids and autonomous vehicles as core applications. His research interests focus on control methods for cyber-physical systems, particularly in the modeling and control of large-scale systems and optimal multi-level information management.

Appendix

A. Auxiliary results

Lemma 1: Consider two vehicles $i,j \in \mathcal{I}_0^N$ with the corresponding sampling sequences Δ_i and Δ_j. Then, for all $t_{k_i} \in \Delta_i$ and $t_{k_{j+1}} \in \Delta_j$ the following holds:

1) if $t_{k_{j+1}} \in [t_{k_i}, t_{k_i+1})$ then

$$t_{k_{i+1}} - t_{k_{j+1}} \leq \tilde{T}, \quad \tilde{T} = \Big(\frac{T_{\max}}{T_{\min}} - 1\Big) T_{\max}; \tag{32}$$

2) if $t_{k_i} \in [t_{k_j}, t_{k_j+1})$ then

$$t_{k_i} - t_{k_j} \leq \hat{T}, \quad \hat{T} = \frac{1}{T_{\min}}(T_{\max}^2 - T_{\min}^2). \tag{33}$$

Proof: To prove 1) we notice that

$$t_{k_{i+1}} \leq t_{k_{j+1}} + \frac{T_{\max}}{T_{\min}} T_j \leq t_{k_{j+1}} + \frac{T_{\max}}{T_{\min}} T_{\max}$$

so getting the result. 2) follows from 1) as $t_{k_i} \leq t_{k_{i+1}}$. ■

Lemma 2: Consider the vehicle dynamics (1) under Assumption 1 with $i \in \mathcal{I}_0^N$ and let (9) be its sampled-data equivalent model. Then, the following inequality holds

$$\|f_i(t_\ell)\| \leq p_d \|d_i\|^{[t_{k_i}, t_{k_i+1})} + p_u \|u_{i-1}(t_\ell)\|^{\{\Delta_{i-1} \cap [t_{k_i}, t_{k_i+1})\}} \tag{34}$$

with $p_u \in \mathbb{R}$ as in (24), setting $T_{\max} = \max_{i \in \mathcal{I}_0^N}\{T_i\}$,

$$p_d := \frac{T_{\max}}{2}\sqrt{T_{\max}^2 + 4}. \tag{35}$$

In addition, if the disturbance $\tilde{d}_i$ verifies (20), then

$$p_d \|d_i\|^{[0, t_{k_i}]} \leq 2 p_d \ \delta_d. \tag{36}$$

Proof: The definition of (10b) yields that

$$\sum_{r=0}^{\mu_i} D_i^r \big(u_{i-1}(t_{k_i}^{r-1}) - u_{i-1}(t_{k_i})\big) = \int_{t_{k_i}^0}^{t_{k_i+1}} e^{A(t_{k_i+1} - s)} B \big(u_{i-1}(s) - u_{i-1}(t_{k_i})\big) \mathrm{d}s.$$

Accordingly, one gets

$$\begin{aligned}\|f_i(t_\ell)\| \leq & \sup_{\ell \in \{0,\dots,k_i\}} |\int_0^{T_i} e^{As} B d_i(t_{\ell+1} - s) \mathrm{d}s| \\ & + |\int_{t_{k_i}^0}^{t_{k_i+1}} e^{A(t_{k_i+1} - s)} B \big(u_{i-1}(s) - u_{i-1}(t_{k_i})\big) \mathrm{d}s| \\ \leq & \sup_{\ell \in \{0,\dots,k_i\}} |\int_0^{T_i} e^{As} B d_i(t_{\ell+1} - s) \mathrm{d}s| \\ & + 2 |\int_{t_{k_i}^0}^{t_{k_i+1}} e^{A(t_{k_i+1} - s)} B \mathrm{d}s| \sup_{r \in \{1,\dots,\mu_i\}} |u_{i-1}(t_{k_i}^{r-1})|.\end{aligned}$$

As far as the first term is concerned, one gets

$$|\int_0^{T_i} e^{As} B d_i(t_{\ell+1} - s) \mathrm{d}s| \leq |\int_0^{T_i} e^{As} B \mathrm{d}s| \|d_i\|^{[t_{k_i}, t_{k_i+1})}.$$

Then, for all $t_2 \geq t_1 > 0$, we notice that

$$\int_{t_1}^{t_2} e^{As} B \mathrm{d}s = (t_2 - t_1) \begin{bmatrix} \frac{t_2 - t_1}{2} \\ 1 \end{bmatrix}. \tag{37}$$

Accordingly, setting $t_1 = 0$, $t_2 = T_i$ and recalling that $T_{\max} = \max_{i \in \mathcal{I}_0^N}\{T_i\}$, one gets

$$|\int_0^{T_i} e^{As} B \mathrm{d}s| = \frac{T_i}{2}\sqrt{T_i^2 + 4} \leq \frac{T_{\max}}{2}\sqrt{T_{\max}^2 + 4}$$

so that (34) holds for the part in d_i. At this point, by definition of $d_i = \tilde{d}_i - \tilde{d}_{i-1}$ one gets

$$\|\tilde{d}_i - \tilde{d}_{i-1}\|^{[t_{k_i}, t_{k_i+1})} \leq \|\tilde{d}_i\|^{[t_{k_i}, t_{k_i+1})} + \|\tilde{d}_{i-1}\|^{[t_{k_i}, t_{k_i+1})}$$

thus yielding (36) if (20) holds. As far as the second term is concerned, it is a direct consequence of (37) and 1) in Lemma 1. ■

Lemma 3: Consider a platoon of N vehicles under the assumptions of Theorem 1. For a given time instant $t_k > 0$ and a vehicle $i \in \mathcal{I}_0^N$, introduce the sequences

$$\begin{aligned}&{}^\ell K_j(t_k) := \{{}^\ell k_1, \dots, {}^\ell k_j\}, \ {}^\ell \bar{K}_j(t_k) := \{{}^\ell \bar{k}_j, \dots, {}^\ell \bar{k}_j\} \\ &{}^\ell K_j^M(t_k) := \{{}^\ell k_1^M, \dots, {}^\ell k_j^M\}, \quad {}^\ell \mathbb{K}_j(t_k) := {}^\ell K_j(t_k) \cup {}^\ell \bar{K}_j(t_k)\end{aligned}$$

and corresponding to the time instants[1]

$$\begin{aligned}t_{\ell k_j}(t_k) &= \max_{t \in \Delta_\ell}\{t \leq t_{\ell+1 k_j} \text{ for } {}^{\ell+1}k_j \in {}^{\ell+1}K_j\} \\ t_{\ell k_j^M}(t_k) &= \max_{t \in \Delta_\ell^M}\{t \leq t_{\ell+1 k_j^M} \text{ for } {}^{\ell+1}k_j^M \in {}^{\ell+1}K_j^M\} \\ t_{i k_i}(t_k) &= \max_{t \in \Delta_i}\{t \leq t_k\}, \quad t_{i k_i^M}(t_k) = \max_{t \in \Delta_i^M}\{t \leq t_k\} \\ t_{\ell \bar{k}_j}(t_k) &= \max_{t \in \Delta_\ell}\{t \leq t_{\ell k_j^M} \text{ for } {}^\ell k_j^M \in {}^\ell K_j^M\}\end{aligned}$$

for all $j, \ell \in \mathcal{I}_0^{i-1}$ such that $\ell < j \leq i$. Then, the following inequalities hold

$$|\zeta_i(t_k)| \leq \sum_{\ell=0}^{i} \Big(a_i^\ell \|\zeta_\ell(t_r)\|^{{}^\ell \mathbb{K}_i} + \delta_i^\ell \|d_\ell(t)\|^{[t_{\ell \bar{k}_i}, t_k)}\Big) \tag{38a}$$

$$|u_i(t_k)| \leq \sum_{\ell=0}^{i} \Big(h_i^\ell \|\zeta_\ell(t_r)\|^{{}^\ell \mathbb{K}_i} + \Gamma_i^\ell \|d_\ell(t)\|^{[t_{\ell \bar{k}_i}, t_k)}\Big) \tag{38b}$$

[1]In the proofs, all dependencies of the sequences and time instants above on t_k will be neglected for the sake of simplicity.

with $h_i^\ell, a_i^\ell \in \mathbb{R}$ defined in (24) and

$$\begin{aligned}\delta_i^\ell &= \begin{cases}\bar{p}_u \Gamma_i^\ell, & \ell \in \{0,\dots,i-1\}\\ \bar{p}_u, & \ell = i\end{cases}\\ \Gamma_i^\ell &= \begin{cases}\kappa \rho_i^{\ell+1}\delta_\ell^\ell, & \ell \in \{0,\dots,i-1\}\\ 0, & \ell = i.\end{cases}\end{aligned} \tag{39}$$

Proof: First of all, we note that by definition of ρ_i in (16) one has that for all $t_k \in [t_{k_i+1}, t_{k_i})$ one has $\rho_i(t_k) = \rho_i(t_{k_i})$ and $u_i(t_k) = u_i(t_{k_i})$ thus yielding, for $\tilde{\chi}_i = \chi_i(t) - \chi_{e,i}$

$$\begin{aligned}\zeta_i(t_k) =& \text{col}\{\tilde{\chi}_i(t),\ \rho(t_{k_i})\}\\ =& \tilde{A}\zeta_i(t_{k_i}) + \text{col}\{\int_{t_{k_i}}^{t_k} e^{A(t_k-s)}B\big(u_i(t_{k_i}) + d(s)\big)\mathrm{d}s,\ 0\}\\ \tilde{A} =& \text{diag}\{e^{A(t_k-t_{k_i})},\ I_{\rho_i}\}.\end{aligned}$$

Accordingly, setting $\tilde{t} = t_k - t_{k_i} \in [0, \tilde{T}]$, one gets

$$|\tilde{A}| = \frac{\sqrt{2}}{2}\sqrt{\tilde{t}\sqrt{\tilde{t}^2+4}+\tilde{t}^2+2}$$

and thus, using 2) in Lemma 1,

$$\begin{aligned}&|\text{col}\{\int_{t_{k_i}}^{t_k} e^{A(t_k-s)}B\big(u_i(t_{k_i}) + d(s)\big)\mathrm{d}s, 0\}|\\ &\quad\le \frac{\tilde{t}}{2}\sqrt{4+\tilde{t}^2}(|u_i(t_{k_i})| + \|d_i(t)\|^{[t_{k_i},t_k]})\\ &\quad\le \bar{p}_u(|u_i(t_{k_i})| + \|d_i(t)\|^{[t_{k_i},t_k]})\end{aligned}$$

with a and $\bar{p}_u$ as in (24). Accordingly, for all $t_k \in [t_{k_i}, t_{k_i+1})$ one gets

$$\begin{aligned}|\zeta_i(t_k)| \le& a|\zeta_i(t_{k_i})| + \bar{p}_u\big(|u_i(t_{k_i})| + \|d_i(t)\|^{[t_{k_i},t_k)}\big)\\ |u_i(t_{k_i})| \le& |u_{i-1}(t_{i-1k_i})| + h_i^i|\zeta_i(t_{k_i})| + r_i|\psi_{i-1}(t_{k_i^M})|\end{aligned}$$

so getting that

$$\begin{aligned}|\zeta_i(t_k)| \le\ & a_i^i|\zeta_i(t_{k_i})| + \bar{p}_u|u_{i-1}(t_{i-1k_i})|\\ &+\bar{p}_u r_i|\psi_{i-1}(t_{k_i^M})| + \delta_i^i\|d_i(t)\|^{[t_{k_i},t_k)}.\end{aligned} \tag{40}$$

In addition, we get that

$$|\psi_{i-1}(t_{k_i^M})| \le \kappa\sum_{\ell=0}^{i-1}|\zeta_\ell(t_{k_i}^M)| = \kappa|\zeta_{i-1}(t_{k_i}^M)| + \kappa\sum_{\ell=0}^{i-2}|\zeta_\ell(t_{k_i}^M)|$$

thus yielding

$$\begin{aligned}|\zeta_i(t_k)| \le& a_i^i|\zeta_i(t_{k_i})| + \bar{p}_u|u_{i-1}(t_{i-1k_i})|\\ &+\bar{p}_u\kappa r_i\sum_{\ell=0}^{i-1}|\zeta_\ell(t_{k_i}^M)| + \delta_i^i\|d_i(t)\|^{[t_{k_i},t_k)}\end{aligned} \tag{41a}$$

$$\begin{aligned}|u_i(t_{k_i})| \le& |u_{i-1}(t_{i-1k_i})| + h_i^i|\zeta_i(t_{k_i})| + r_i\kappa\sum_{\ell=0}^{i-1}|\zeta_\ell(t_{k_i}^M)|.\end{aligned} \tag{41b}$$

Accordingly, exploiting (40) with $i-1 \mapsto i$, $t_{k_i^M} \mapsto t_k$ and $t_{i-1k_i^M} \mapsto t_{k_i^M}$ and *mutatis mutandis* for the rest, one gets

$$\begin{aligned}|\zeta_{i-1}(t_{k_i}^M)| \le& a_{i-1}^{i-1}|\zeta_{i-1}(t_{i-1\bar{k}_i})| + \bar{p}_u|u_{i-2}(t_{i-1\bar{k}_{i-1}})|\\ &+\bar{p}_u r_{i-1}|\psi_{i-2}(t_{i-1k_i^M})|\\ &+\delta_{i-1}^{i-1}\|d_{i-1}(t)\|^{[t_{i-1\bar{k}_i},t_k)}.\end{aligned}$$

As far as $u_{i-1}(t_{i-1k_i})$ in (40) is concerned, one gets

$$\begin{aligned}|u_{i-1}(t_{i-1k_i})| \le& |u_{i-2}(t_{i-2k_i})|\\ &+h_{i-1}^{i-1}|\zeta_{i-1}(t_{i-1k_i})| + r_{i-1}|\psi_{i-2}(t_{i-1k_i^M})|\\ \le& |u_{i-2}(t_{i-2k_i})|\\ &+h_{i-1}^{i-1}|\zeta_{i-1}(t_{i-1k_i})| + r_{i-1}\kappa\sum_{\ell=0}^{i-2}|\zeta_\ell(t_{i-1k_i^M})|\end{aligned}$$

thus yielding

$$\begin{aligned}&|u_{i-1}(t_{i-1k_i})| + \kappa r_i|\zeta_{i-1}(t_{k_i}^M)|\\ &\le h_i^{i-1}\|\zeta_{i-1}(t_r)\|^{i-1\mathbb{K}_i} + \sigma_i^{i-1}\|u_{i-2}(t_r)\|^{i-1\mathbb{K}_i}\\ &+ r_{i-1}\sigma_i^{i-1}\|\psi_{i-2}(t_r)\|^{i-1\mathbb{K}_i^M} + \Gamma_i^{i-1}\|d_{i-1}(t)\|^{[t_{i-1\bar{k}_i},t_k)}.\end{aligned}$$

Substituting the relation above into (41b) yields

$$\begin{aligned}|u_i(t_{k_i})| \le& \sum_{\ell=i-1}^{i}\Big(h_i^\ell\|\zeta_\ell(t_r)\|^{\ell\mathbb{K}_i} + \Gamma_i^\ell\|d_\ell(t)\|^{[t_{\ell\bar{k}_i},t_k)}\Big)\\ &+\sigma_i^{i-1}\|u_{i-2}(t_r)\|^{i-1\mathbb{K}_i} + r_{i-1}\sigma_i^{i-1}\|\psi_{i-2}(t_r)\|^{i-1\mathbb{K}_i^M}\\ &+\kappa r_i\sum_{\ell=0}^{i-2}|\zeta_\ell(t_{k_i}^M)|\\ \le& \sum_{\ell=i-1}^{i}\Big(h_i^\ell\|\zeta_\ell(t_r)\|^{\ell\mathbb{K}_i} + \Gamma_i^\ell\|d_\ell(t)\|^{[t_{\ell\bar{k}_i},t_k)}\Big)\\ &+\sigma_i^{i-1}\|u_{i-2}(t_r)\|^{i-1\mathbb{K}_i} + \kappa\varsigma_i^{i-1}\sum_{\ell=0}^{i-2}\|\zeta_\ell(t_r)\|^{\ell\mathbb{K}_i^M}.\end{aligned}$$

Accordingly, (41a) reads

$$\begin{aligned}|\zeta_i(t_k)| \le& \sum_{\ell=i-1}^{i}\Big(a_i^\ell\|\zeta_i(t_r)\|^{\ell\mathbb{K}_i} + \delta_i^\ell\|d_\ell(t)\|^{[t_{\ell\bar{k}_i},t_k)}\Big)\\ &+\bar{p}_u\sigma_i^{i-1}\|u_{i-2}(t_r)\|^{i-1\mathbb{K}_i} + \bar{p}_u\kappa\varsigma_i^{i-1}\sum_{\ell=0}^{i-2}\|\zeta_\ell(t_r)\|^{\ell\mathbb{K}_i^M}.\end{aligned}$$

Along the same lines, collecting in the inequalities above all terms in $i-2 \in \mathcal{I}_0^N$, one gets

$$\begin{aligned}&\sigma_i^{i-1}\|u_{i-2}(t_r)\|^{i-1\mathbb{K}_i} + \kappa\varsigma_i^{i-1}\|\zeta_{i-2}(t_r)\|^{i-2\mathbb{K}_i^M}\\ &\le h_i^{i-2}\|\zeta_{i-2}(t_r)\|^{i-2\mathbb{K}_i} + \sigma_i^{i-2}\|u_{i-3}(t_r)\|^{i-2\mathbb{K}_i}\\ &+ r_{i-2}\sigma_i^{i-2}\|\psi_{i-3}(t_r)\|^{i-1\mathbb{K}_i^M} + \Gamma_i^{i-2}\|d_{i-2}(t)\|^{[t_{i-2\bar{k}_i},t_k)}\end{aligned}$$

thus yielding

$$\begin{aligned}|u_i(t_{k_i})| \le& \sum_{\ell=i-2}^{i}\Big(h_i^\ell\|\zeta_\ell(t_r)\|^{\ell\mathbb{K}_i} + \Gamma_i^\ell\|d_\ell(t)\|^{[t_{\ell\bar{k}_i},t_k)}\Big)\\ &+\sigma_i^{i-2}\|u_{i-3}(t_r)\|^{i-2\mathbb{K}_i} + \kappa\varsigma_i^{i-2}\sum_{\ell=0}^{i-3}\|\zeta_\ell(t_r)\|^{\ell\mathbb{K}_i^M}\\ |\zeta_i(t_k)| \le& \sum_{\ell=i-2}^{i}\Big(a_i^\ell\|\zeta_i(t_r)\|^{\ell\mathbb{K}_i} + \delta_i^\ell\|d_\ell(t)\|^{[t_{\ell\bar{k}_i},t_k)}\Big)\\ &+\bar{p}_u\sigma_i^{i-2}\|u_{i-3}(t_r)\|^{i-2\mathbb{K}_i} + \bar{p}_u\kappa\varsigma_i^{i-2}\sum_{\ell=0}^{i-3}\|\zeta_\ell(t_r)\|^{\ell\mathbb{K}_i^M}.\end{aligned}$$

Going on iteratively one gets the result. ■

Lemma 4: Consider a platoon of N vehicles under the assumptions of Theorem 1. For all $i \in \mathcal{I}_0^N$, pick $t_{k_i} = k_i T_i \in \Delta_i$ and $t_{k_i^M} = m k_i T_i^M \in \Delta_i^M$ with the property that $t_{k_i^M} \leq t_{k_i}$. Then, rewriting $k_i = m k_i^M + \bar{k}_i$, $\bar{k}_i \in \{0, 1, \ldots, m-1\}$ and denoting $\boldsymbol{F}_{m,i} = (I - F_i)^{-1}(I - F_i^m)$, the explicit dynamics of each $i \in \mathcal{I}_0^N$ is given by

$$\begin{aligned}\zeta_i(t_{k_i}) =& F_i^{k_i}\zeta_i(0) + \sum_{\ell=0}^{k_i-1} F_i^{(k_i-1-\ell)} E f_i(t_\ell) \\ &+ \boldsymbol{F}_{m,i} \sum_{\ell=0}^{k_i^M} F^{k_i^M-(\ell+1)m} G_i \psi_{i-1}(t_\ell) \\ &+ \boldsymbol{F}_{\bar{k}_i,i} G_i \psi_{i-1}(t_{k_i^M}).\end{aligned} \tag{42}$$

Proof: The proof follows by computing

$$\begin{aligned}\zeta_i(t_{k_i}) =& F_i^{k_i}\zeta_i(0) + \sum_{\ell=0}^{k_i-1} F_i^{(k_i-1-\ell)} E f_i(t_\ell) \\ &+ \sum_{\ell=0}^{k_i^M} \sum_{\bar{r}=\ell m}^{(\ell+1)m-1} F_i^{k_i-1-\bar{r}} G_i \psi_{i-1}(t_\ell) \\ &+ \sum_{\bar{r}=m k_i^M}^{k_i-1} F_i^{k_i-1-\bar{r}} G_i \psi_{i-1}(t_{k_i^M}).\end{aligned} \tag{43}$$

One sets $r = (\ell+1)m - 1 - \bar{r}$ in the term below

$$\begin{aligned}\sum_{r=\ell m}^{(\ell+1)m-1} F_i^{k_i-1-r} =& F_i^{k_i-(\ell+1)m} \sum_{r=0}^{m-1} F_i^r \\ =& F_i^{k_i-(\ell+1)m}(I - F_i)^{-1}(I - F^m) \\ =& (I - F_i)^{-1}(I - F_i^\mu) F_i^{k_i-(\ell+1)m}.\end{aligned} \tag{44}$$

Similarly, setting $r = k_i - 1 - \bar{r}$ in the term below one gets

$$\sum_{\bar{r}=m k_i^M}^{k_i-1} F_i^{k_i-1-\bar{r}} = \sum_{r=0}^{\bar{k}_i-1} F_i^r = (I - F_i)^{-1}(I - F_i^{\bar{k}_i})$$

and, thus, the result. ∎

B. Proof of Theorem 1

For all $i \in \mathcal{I}_0^N$, the platoon gets the cascaded form

$$\begin{aligned}\zeta_0(t_{k_0+1}) &= F_0\zeta_0(t_{k_0}) + E f_0(t_{k_0}) \\ &\vdots \\ \zeta_i(t_{k_i+1}) &= F_i\zeta_i(t_{k_i}) + G_i\psi_{i-1}(\zeta_0(t_{k_i^M}), \ldots, \zeta_{i-1}(t_{k_i^M})) \\ &\quad + E f_i(t_{k_i}).\end{aligned} \tag{45}$$

We proceed in two steps to prove, in order, (i) string stability; (ii) disturbance string stability (and, thus, asymptotic string stability as well).

(i) **String stability.** We proceed iteratively and by induction by considering the leader and the first vehicle (i.e., $i = 0$ and $i = 1$) at first. Recalling that $t_{k_0} = k_0 T_0$, for all initial conditions $\zeta_0(0) \in \mathbb{R}^{2+n_\eta}$, the corresponding trajectories are given by

$$\zeta_0(t_{k_0}) = F_0^{k_0}\zeta_0(0) + \textstyle\sum_{\ell=0}^{k_0-1} F_0^{(k_0-1-\ell)} E f_0(t_\ell).$$

By 1), all F_is are Schur stable and, thus, the leader is exponentially stable so that fixing $\beta_0 > 0$ and $\alpha_0 \in (0,1)$ yields $|F_0^{k_0}| \leq \beta_0 {\alpha_0}^{k_0}$ and thus

$$\begin{aligned}|\zeta_0(t_{k_0})| \leq& \beta_0 {\alpha_0}^{k_0}|\zeta_0(0)| + \frac{\beta_0}{1-\alpha_0}\|f_0(t_\ell)\|^{\{0,\ldots,k_0\}} \\ \leq& \beta_0|\zeta_0(0)| + \beta_0\eta_0^0\|d_0(t_\ell)\|^{\{0,\ldots,k_0\}}\end{aligned}$$

when defining $\eta_0^0 = p_d\,(1-\alpha_0)^{-1}$. Consider now $i = 1$. Exploiting Lemma 4, for all initial conditions $\zeta_1(0) \in \mathbb{R}^{2+n_\eta}$ the corresponding trajectory rewrites as (43). Thus, as per the previous case, by virtue of 1), one has that $|F_1^{k_1}| \leq \beta_1 {\alpha_1}^{k_1}$ so yielding, exploiting Lemma 2 and [43],

$$\begin{aligned}|\zeta_1(t_{k_1})| \;\leq\; & \beta_1 {\alpha_1}^{k_1}|\zeta_1(0)| + \tfrac{\beta_1}{1-\alpha_1}|G_i|\|\psi_0(\zeta_0(t_\ell))\|^{\{0,\ldots,k_1^M\}} \\ & + \tfrac{\beta}{1-\alpha_1}\|f_1(t_\ell)\|^{\{0,\ldots,k_1\}} \\ \leq\; & \beta_1 {\alpha_1}^{k_1}|\zeta_1(0)| + \tfrac{\beta_1 g_1}{1-\alpha}\|\psi_0(\zeta_0(t_\ell))\|^{\{0,\ldots,k_1^M\}} \\ & + \tfrac{\beta_1}{1-\alpha_1}\Big(p_d\|d_1(t)\|^{[0,t_{k_1}]} + p_u\|u_0(t_\ell)\|^{\{0,\ldots,k_1\}}\Big).\end{aligned}$$

At this point, combining (14), (38a) and (38b) with $t_{k_0} = \max_{t\in\Delta_0}\{t \leq t_{k_1}\}$ yields

$$\begin{aligned}\|\psi_0(\zeta_0(t_\ell))\|^{\{0,\ldots,k_1^M\}} \leq& \kappa\|\zeta_0(t_\ell)\|^{\{0,\ldots,k_1^M\}} \\ \leq& \kappa\big(a_0^0\|\zeta_0(t_\ell)\|^{\{0,\ldots,k_0\}} + \delta_0^0\|d_0(t)\|^{[0,t_{k_1}]}\big) \\ \|u_0(t_\ell)\|^{\{0,\ldots,k_1\}} \leq& h_0^0\|\zeta_0(t_\ell)\|^{\{0,\ldots,k_0\}} + \delta_0^0\|d_0(t)\|^{[0,t_{k_1}]}\end{aligned}$$

so getting

$$\begin{aligned}|\zeta_1(t_{k_1})| \leq& \beta_1 {\alpha_1}^{k_1}|\zeta_1(0)| \\ &+ \frac{\beta_1}{1-\alpha_1}\big(h_0^0 p_u + \kappa g_1 a_0^0\big)\|\zeta_0(t_\ell)\|^{\{0,\ldots,k_0\}} \\ &+ \frac{\beta_1}{1-\alpha_1}\Big(p_d\|d_1(t)\|^{[0,t_{k_1}]} \\ &+ (p_u\Gamma_0^0 + \kappa g_1\delta_0^0)\|d_0(t)\|^{[0,t_{k_1}]}\Big) \\ \leq& \beta_1 {\alpha_1}^{k_1}|\zeta_1(0)| + \beta_1\gamma_1\big(|\zeta_0(0)|\big) \\ &+ \beta_1\Big(\eta_1^1\|d_1(t)\|^{[0,t_{k_1}]} + \eta_1^0\|d_0(t)\|^{[0,t_{k_1}]}\Big) \\ \leq& \beta_1(1+\gamma_1)\max_{\ell\in\mathcal{I}_0^i}\{\big(|\zeta_\ell(0)|\big)\} \\ &+ \beta_1\Big(\eta_1^1\|d_1(t)\|^{[0,t_{k_1}]} + \eta_1^0\|d_0(t)\|^{[0,t_{k_1}]}\Big) \\ \leq& \beta_1(1+\gamma)\max_{\ell\in\mathcal{I}_0^i}\{\big(|\zeta_\ell(0)|\big)\} + \beta_1\sum_{\ell=0}^{1}\eta_1^\ell\|d_\ell(t)\|^{[0,t_{k_1}]}\end{aligned}$$

by definition of (23) and denoting

$$\begin{aligned}&\eta_1^1 = p_d\,(1-\alpha_1)^{-1}, \quad \eta_1^0 = \nu_1^0 + \bar{\gamma}_1^0\eta_0^0 \\ &\gamma_1 = \bar{\gamma}_1^0 = (1-\alpha_1)^{-1}\big(h_0^0 p_u + \kappa g_1 a_0^0\big)\beta_0. \\ &\bar{\nu}_1^0 = (1-\alpha_0)^{-1}\big(\Gamma_0^0 p_u + \kappa g_1\bar{\delta}_0^0\big).\end{aligned}$$

It is clear that, setting $d_1 \equiv 0$ and because $\gamma \in (0,1)$ string stability holds when restricted to the leader and

the first vehicle. Let us proceed now by induction and let us consider the i^{th} vehicle. Then, one gets

$$\begin{aligned}|\zeta_i(t_{k_i})| \leq&\beta_i{\alpha_i}^{k_i}|\zeta_i(0)| + \frac{\beta_i}{1-\alpha_i}\|f_i(t_\ell)\|^{\{0,\dots,k_i\}}\\ &+\frac{\beta_i}{1-\alpha_i}g\|\psi_{i-1}(\zeta_0(t_\ell),\dots,\zeta_{i-1}(t_\ell))\|^{\{0,\dots,k_i^M\}}\\ \leq&\beta_i{\alpha_i}^{k_i}|\zeta_i(0)|\\ &+\frac{\beta_i}{1-\alpha_i}g\|\psi_{i-1}(\zeta_0(t_\ell),\dots,\zeta_{i-1}(t_\ell))\|^{\{0,\dots,k_i^M\}}\\ &+\frac{\beta_i}{1-\alpha_i}\big(p_d\|d_i(t)\|^{[0,t_{k_i}]}+p_u\|u_{i-1}(t_\ell)\|^{\{0,\dots,t_{k_i}\}}\big).\end{aligned}$$

Combining (14) and (38a) with $t_{k_\ell} = \max_{t\in\Delta_\ell}\{t \leq t_{k_i}\}$ yields, with $\bar a_{i-1}^\ell$ and $\bar\delta_{i-1}^\ell$ as in (24),

$$\begin{aligned}&\|\psi_{i-1}(\zeta_0(t_\ell),\dots,\zeta_{i-1}(t_\ell))\|^{\{0,\dots,k_i^M\}}\\ &\quad\leq\kappa\sum_{\ell=0}^{i-1}\|\zeta_\ell(t_\ell)\|^{\{0,\dots,k_i^M\}} \leq \kappa\sum_{\ell=0}^{i-1}\|\zeta_\ell(t_\ell)\|^{\{0,\dots,k_i\}}\\ &\quad\leq\kappa\sum_{\ell=0}^{i-1}\Big(\bar a_{i-1}^\ell\|\zeta_\ell(t_\ell)\|^{\{0,\dots,k_\ell\}}+\bar\delta_{i-1}^\ell\|d_\ell(t)\|^{[0,t_{k_i}]}\Big).\end{aligned}$$

Exploiting now (38b) one gets

$$\begin{aligned}|\zeta_i(t_{k_i})| \leq&\beta_i{\alpha_i}^{k_i}|\zeta_i(0)| + \frac{\beta_i}{1-\alpha_i}p_d\|d_i(t)\|^{[0,t_{k_i}]}\\ &+\frac{\beta_i}{1-\alpha_i}\sum_{\ell=0}^{i-1}(h_{i-1}^\ell p_u+\kappa g_i\bar a_{i-1}^\ell)\|\zeta_\ell(t_\ell)\|^{\{0,\dots,k_\ell\}}\\ &+\frac{\beta_i}{1-\alpha_i}\sum_{\ell=0}^{i-1}(\Gamma_{i-1}^\ell p_u+\kappa g_i\bar\delta_{i-1}^\ell)\|d_\ell(t)\|^{[0,t_{k_i}]}.\end{aligned}$$

Assuming that for all $\ell\in\mathcal{I}_0^{i-1}$ the relation below holds

$$\begin{aligned}|\zeta_\ell(t_{k_\ell})| \leq&\beta_\ell(1+\dots+\gamma^\ell)\max_{j\in\mathcal{I}_0^\ell}\{|\zeta_j(0)|\}\\ &+\beta_\ell\sum_{j=0}^{\ell}\eta_\ell^j\|d_j(t)\|^{[0,t_{k_i}]}\end{aligned}$$

for some η_ℓ^j to define later on and

$$\begin{aligned}&\bar\gamma_i^\ell = (1-\alpha_i)^{-1}\left(h_{i-1}^\ell p_u+\kappa g_i\bar a_{i-1}^\ell\right)\beta_\ell\\ &\bar\nu_i^\ell = (1-\alpha_i)^{-1}\left(\Gamma_{i-1}^\ell p_u+\kappa g_i\bar\delta_{i-1}^\ell\right),\quad \sigma_i^{i-1} = p_d\,(1-\alpha_i)^{-1}\end{aligned}$$

one gets

$$\begin{aligned}|\zeta_i(t_{k_i})| \leq&\beta_i{\alpha_i}^{k_i}|\zeta_i(0)|\\ &+\beta_i\sum_{\ell=0}^{i-1}\bar\gamma_i^\ell(1+\dots+\gamma^\ell)\max_{j\in\mathcal{I}_0^\ell}\{|\zeta_j(0)|\}\\ &+\beta_i\sum_{\ell=0}^{i-1}\bar\gamma_i^\ell\sum_{j=0}^{\ell}\eta_\ell^j\|d_j(t)\|^{[0,t_{k_i}]}\\ &+\beta_i\sum_{\ell=0}^{i-1}\bar\nu_i^\ell\|d_\ell(t)\|^{[0,t_{k_i}]}+\beta_i\sigma_i^{i-1}\|d_i(t)\|^{[0,t_{k_i}]}.\end{aligned}$$

At this point, by definition of (23) one gets that

$$\sum_{\ell=0}^{i-1}\bar\gamma_i^\ell(1+\dots+\gamma^\ell)\leq\gamma+\dots+\gamma^i$$

and thus, suitably regrouping terms in $\|d_\ell(t)\|$

$$\begin{aligned}|\zeta_i(t_{k_i})| \leq&\beta_i(1+\dots+\gamma^i)\max_{\ell\in\mathcal{I}_0^i}\{|\zeta_\ell(0)|\}\\ &+\beta_i\sum_{\ell=0}^{i}\eta_i^\ell\|d_\ell(t)\|^{[0,t_{k_i}]}\end{aligned}$$

with

$$\eta_i^\ell = \begin{cases}\bar\nu_i^\ell+\sum_{j=\ell}^{i-1}\bar\gamma_i^j\eta_j^\ell, & \ell\in\{0,\dots,i-1\}\\ \frac{p_d}{1-\alpha_i} & \ell=i.\end{cases}$$

Since $\gamma\in(0,1)$ one gets $1+\dots+\gamma^i\leq(1-\gamma)^{-1}$ and

$$\begin{aligned}|\zeta_i(t_{k_i})| \quad\leq\quad&\beta_i\,(1-\gamma)^{-1}\max_{\ell\in\mathcal{I}_0^i}\{|\zeta_\ell(0)|\}\\ &+\Big(\beta_i\textstyle\sum_{\ell=0}^{i}\eta_i^\ell\Big)\sup_{\ell\in\mathcal{I}_0^i}\{\|d_\ell(t)\|^{[0,t_{k_i}]}\}.\end{aligned}$$

Fixing $\tilde d_i\equiv 0$ for all $i\in\mathcal{I}_0^N$ and $\beta=\max_{i\in\mathcal{I}_0^N}\{\beta_i\}$, the inequality below holds for all $t_{k_i}\in\Delta_i$ and $t_{k_i^M}\in\Delta_i^M$

$$\max_{i\in\mathcal{I}_0^N}|\zeta_i(t_{k_i})| \quad\leq\quad (1-\gamma)^{-1}\,\beta\max_{i\in\mathcal{I}_0^N}\{|\zeta_j(0)|\}.$$

Thus, string stability holds in the sense of Definition 2 as for all $\varepsilon>0$ one can fix $\varepsilon=(1-\gamma)^{-1}\beta\delta$ and thus $\delta=\beta^{-1}(1-\gamma)\,\varepsilon$.

(*ii*) **Disturbance string stability.** Consider now $\tilde d_i\neq 0$ and verifying (20). Exploiting [44], by the cascade structure of (45), hypothesis 1) and by (14), the transformation

$$\bar\zeta_i(t_{k_i}) = \zeta_i(t_{k_i})+\sum_{\ell=0}^{k_i-1}F_i^{k_i-1-\ell}\Big(E\tilde\psi_{i-1}(t_\ell)+\sum_{r=0}^{\mu_i}\bar D_i^r u_{i-1}(t_\ell^r)\Big)$$

with $\bar D_i^r=\text{col}\{D_i^r,0\}$ and $\tilde\psi_{i-1}(t_{k_i})$ as in (28) is well-defined. Thus, the dynamics of each $i\in\mathcal{I}_0^N$ reads

$$\bar\zeta_i(t_{k_i+1}) = F_i\bar\zeta_i(t_{k_i})+E\int_0^{T_i}e^{As}Bd_i(t_{k_i+1}-s)\text{d}s. \quad (46)$$

In the new coordinates, it is clear that when $\tilde d_i\equiv 0$, each vehicle is exponentially stable. This, together with string stability, proves asymptotic string stability in the sense of Definition 1. As far as disturbance string stability is concerned, 1) and Lemma 2 yield

$$|\bar\zeta_i(t_{k_i})|\leq\beta\alpha^{k_i}\bar\zeta_i(0)+2\,(1-\alpha)^{-1}\,\beta p_d\delta_d$$

with $\alpha=\max i\in\mathcal{I}_0^N\{\alpha_i\}$. Thus the proof is concludes as one gets for all $t_k^i\in\Delta_i$ and all $i\in\mathcal{I}_0^N$ that

$$\begin{aligned}\max_{i\in\mathcal{I}_0^N}\{|\bar\zeta_i(t_{k_i})|\}\leq\quad&\beta\alpha^{k_i}\max_{i\in\mathcal{I}_0^N}\{|\bar\zeta_i(0)|\}\\ &+2\,(1-\alpha)^{-1}\,\beta p_d\delta_d.\end{aligned}$$